





Article

Spatio-Temporal Variation in Landforms and Surface Urban Heat Island in Riverine Megacity

Namita Gorai ¹, Jatisankar Bandyopadhyay ¹, Bijay Halder ^{2,3} , Minhaz Farid Ahmed ⁴ , Altaf Hossain Molla ^{5,*}  and Thomas M. T. Lei ^{6,*} 

¹ Department of Remote Sensing and GIS, Vidyasagar University, Midnapore 721102, India; namitagorai2000@gmail.com (N.G.); jatib@mail.vidyasagar.ac.in (J.B.)

² Department of Earth Sciences and Environment, Faculty of Sciences and Technology, Universiti Kebangsaan Malaysia (UKM), Bangi 43600, Selangor, Malaysia; halder06bijay@gmail.com

³ New Era and Development in Civil Engineering Research Group, Scientific Research Center, Al-Ayen University, Nasiriyah 64001, Iraq

⁴ Institute for Environment and Development (LESTARI), Universiti Kebangsaan Malaysia (UKM), Bangi 43600, Selangor, Malaysia; minhaz@ukm.edu.my

⁵ Department of Mechanical and Manufacturing Engineering, Faculty of Engineering and Built Environment, Universiti Kebangsaan Malaysia (UKM), Bangi 43600, Selangor, Malaysia

⁶ Institute of Science and Environment, University of Saint Joseph, Macau, China

* Correspondence: altafhossain1994@gmail.com (A.H.M.); thomas.lei@usj.edu.mo (T.M.T.L.)

Abstract: Rapid urbanization and changing climatic procedures can activate the present surface urban heat island (SUHI) effect. An SUHI was considered by temperature alterations among urban and rural surroundings. The urban zones were frequently warmer than the rural regions because of population pressure, urbanization, vegetation insufficiency, industrialization, and transportation systems. This investigation analyses the Surface-UHI (SUHI) influence in Kolkata Municipal Corporation (KMC), India. Growing land surface temperature (LST) may cause an SUHI and impact ecological conditions in urban regions. The urban thermal field variation index (UTFVI) served as a qualitative and quantitative barrier to the SUHI susceptibility. The maximum likelihood approach was used in conjunction with supervised classification techniques to identify variations in land use and land cover (LULC) over a chosen year. The outcomes designated a reduction of around 1354.86 Ha, 653.31 Ha, 2286.9 Ha, and 434.16 Ha for vegetation, bare land, grassland, and water bodies, correspondingly. Temporarily, from the years 1991–2021, the built-up area increased by 4729.23 Ha. The highest LST increased by around 7.72 °C, while the lowest LST increased by around 5.81 °C from 1991 to 2021. The vegetation index and LST showed a negative link, according to the correlation analyses; however, the built-up index showed an experimentally measured positive correlation. This inquiry will compel the administration, urban planners, and stakeholders to observe humanistic activities and thus confirm sustainable urban expansion.

Keywords: climate change; ecological disturbance; heat island; urban environment; remote sensing and GIS



Citation: Gorai, N.; Bandyopadhyay, J.; Halder, B.; Ahmed, M.F.; Molla, A.H.; Lei, T.M.T. Spatio-Temporal Variation in Landforms and Surface Urban Heat Island in Riverine Megacity. *Sustainability* **2024**, *16*, 3383. <https://doi.org/10.3390/su16083383>

Academic Editors: Jun Qin and Hou Jiang

Received: 7 March 2024

Revised: 13 April 2024

Accepted: 15 April 2024

Published: 18 April 2024



Copyright: © 2024 by the authors. Licensee MDPI, Basel, Switzerland. This article is an open access article distributed under the terms and conditions of the Creative Commons Attribution (CC BY) license (<https://creativecommons.org/licenses/by/4.0/>).

1. Introduction

With increasing industrialization, urbanization, and population growth, the biological landscapes have been deformed into impermeable surfaces related to building structures, apartments, roads, parking lots, and urban infrastructure [1,2]. It is established that land surface imperviousness was a dangerous constituent influence on the quality of the urban environment [3,4]. Consequently, a significant portion of Kolkata's natural catchment parts have been developed into urban areas. This urbanization process has altered the physical features of the land's surface, including soil moisture, heat transfer efficiency, thermodynamic irradiance characteristics, and albedo. Variations in the land surface temperature (LST) have the greatest ecological impact since they directly affect human

comfort levels, air quality, building energy demand, convective, and latent heat transfer procedures [5–8]. The LST has measured the surface temperature values of the Earth's crust, where reflectance values are observed through space-based observation. Many investigators worldwide have used LST widely in LULC modification assessments to ascertain environmental issues of a particular area [9–12].

Due to the dynamics of green spaces, water scarcity, soil moisture loss, low infiltration rate, and erosion, the urban heat differential has a significant influence on how susceptible an urban environment is [13–15]. Along with environmental degradation, human activities and global climate conditions have significantly affected resident and global land adjustment [16–18]. In the urban region, health subjects like lung cancer, asthma, skin disorders, respiratory ailments, and other health-related challenges were also common [19]. Urban areas are also often the site of additional pollution-related issues as well as the SUHI result [20–22]. The SUHI is an index to identify the heat island effects on the Earth's surface with the help of LST and some methods. This technique is applied to build a heat island effects study and implement awareness and strategies. The SUHI causes pollutants and lowers the air quality in the urban region, which has an impact on the surrounding natural environment and local urban ecology. Due to SUHI stress, SUHIs not only impair human health but also have the potential to increase death rates [23]. In urban areas like Kolkata, the transportation and public industries contributed to air pollution [24]. In this scenario, proper urban management and planning provided further advantages for sustainable growth.

According to some investigation results, the single channel (SC) technique has the lowest accuracy, and the split window (SW) algorithm has reasonable accuracy. Still, LST, overturned from the radiative transfer equation-based technique applying band 10, has the highest inaccuracy with an RMSE lower than 1K [25]. By cross-referencing and linking the Moderate Resolution Imaging Spectroradiometer (MODIS) with Geostationary Ocean Color Imager (GOCI)-derived NDVIs in addition to in situ NDVI dimensions, the researcher evaluated the Landsat 8 OLI/TIRS-derived NDVI characteristics in contrast to Landsat 7 ETM+ [26]. The reproductions of surface reflectance and Top of Atmosphere (TOA) reflectance of broadleaf water and trees are shown for the Landsat 8 OLI/TIRS, MODIS, and Landsat 7 ETM+, to appraise the influence of bandpass alteration on the NDVI calculation [27]. The NDVI is a space-based vegetation monitoring method to identify the green space available on the Earth's surface through different bands in the satellite.

Another examination outcome designates how the stretched (or 'universal') triangle can be applied to understand pixel outlines inside the triangle, and presents how the temporal trajectories of opinions exclusively designate decorations of the LULC change [28]. Finally, we conclude the research with a succinct assessment of the limitations of the method. According to some scientists, over the last 27 years, the built-up zone of Ismailia has gradually increased. The areas with the highest surface radiant temperatures are the barren land (37.34 °C in 1984 and 42.801 °C in 2011) and the built-up region (37.65 °C in 1984 and 43.876 °C in 2011). Vegetated surfaces (28.73 °C in 1984 and 32.96 °C in 2011) have the lowest surface radiant temperatures [29]. The investigation revealed a strong agreement between the real-time ground and satellite RS datasets, with correlation coefficient (R^2) values of 0.90 [30]. The 28-year period (1984–2011) saw significant variations in LST in the Salt Lake Basin area, with an estimated 2 °C shift. This was revealed using themed catalogue diagrams created from remotely sensed and modified satellite imagery.

Urban regions progressively established the amenity's expansion with high reduction buildings. Those belongings were mostly additionally impactful for activating the SUHI effects over the examining area. The UTFVI was also applied to calculate the ecological diversification identified through LST datasets and the notified formulation. Kolkata Municipal Corporation (KMC) progressively documented high green space losses because of urban expansion. Those belongings are likewise triggering land subsidence-related

difficulties with high groundwater shortages. Consequently, the SUHI examination and green space examination are essential for improved urban planning. Current results also showed that, during the summer, Delhi's heavily populated metropolitan area has a greater thermal inertia than the nearby rural areas [31]. The main research gap in this area is in the details of SUHI analysis with ecological variation. Most of the studies applied a ten-year gap of UHI analysis or only LULC-related analysis. In addition, this examination applied a five-year gap-wise landforms analysis with surface temperature measurement and heat island studies. The accuracy assessment of the classification maps and year-wise change detection was also applied to identify the landform alteration in the KMC area. Gradually, different geo-spatial indices with five-year information provide more landform alteration-related evidence. The built-up land, water, soil moisture, bareness analysis, and vegetation scenarios are useful for planning details, management, and novel adaptation strategies toward sustainable urban development. The spatial fluctuation in thermal inertia over the region is starting to make sense of the presence of the Cool Island during the day. The primary goal of this study is to use statistical modelling and RS-based datasets to determine the decadal LULC modification of Kolkata's megacity. The outcomes of this investigation include (a) imageries (LULC) classification from 1991 to 2021 with built-up expansion and vegetation losses; (b) the LST approximation for the thermal condition measurement with SUHI and UTFVI alteration examination; (c) certain geo-spatial indicators for ecological and the environmental impact assessment. These examinations may help the local planners with forthcoming management planning and adaptation strategies to shelter the megacity's environment.

2. Materials and Methods

2.1. Study Area

The British Empire and the East India Company founded the imperial metropolis of Kolkata. The British Indian Empire had its capital at the megacity of Kolkata until 1911 when it was moved to Delhi. To grow the second metropolis of the British Indian Empire, this megacity was created quickly in the 19th century. This was addressed through the fusion of Arabian tradition with Indian philosophy in cultural development. Kolkata is also well known for its creative past, which spans from India to trade the union, and Marxist Naxalite movements. Kolkata, also known as the "City of Palaces", "Cultural Capital of India", "City of Joy", and "The City of Processions", has also been the residence of prominent politicians and yogis. The pandemic that struck Kolkata in 1653 brought with it challenges associated with hasty urbanization, and the city's remnants serve as a model for the urbanization initiatives of less developed countries. The monthly mean temperatures are 19–30 °C (66–86 °F); the annual mean temperature is roughly 26.8 °C (80.2 °F). The summer months of March through June are hot and muggy, with highs in the low 30s; during periods of drought, the highest temperatures ever recorded were higher than 40 °C (104 °F) in May and June (Figure 1). The highest known temperature is around 43.9 °C (111.0 °F), and the lowest is around 5 °C (41 °F). The southwest summer monsoon's Bay of Bengal branch brought rainfall to Kolkata between June and September, giving the city its highest annual precipitation total of roughly 1850 mm (73 in). The provisional Census of India says that 4,496,694 people were living in this megacity in 2011; 2,356,766 of those people were female and 2,139,928 were male. Despite having a megacity population of 4,496,694, Kolkata has an urban/metropolitan population of around 14,035,959, with 6,784,051 women and 7,251,908 men. The oldest disruptive mass transit system in India is the Kolkata Metro, which was developed in 1984. Kolkata, a megacity, has five long-distance lines.

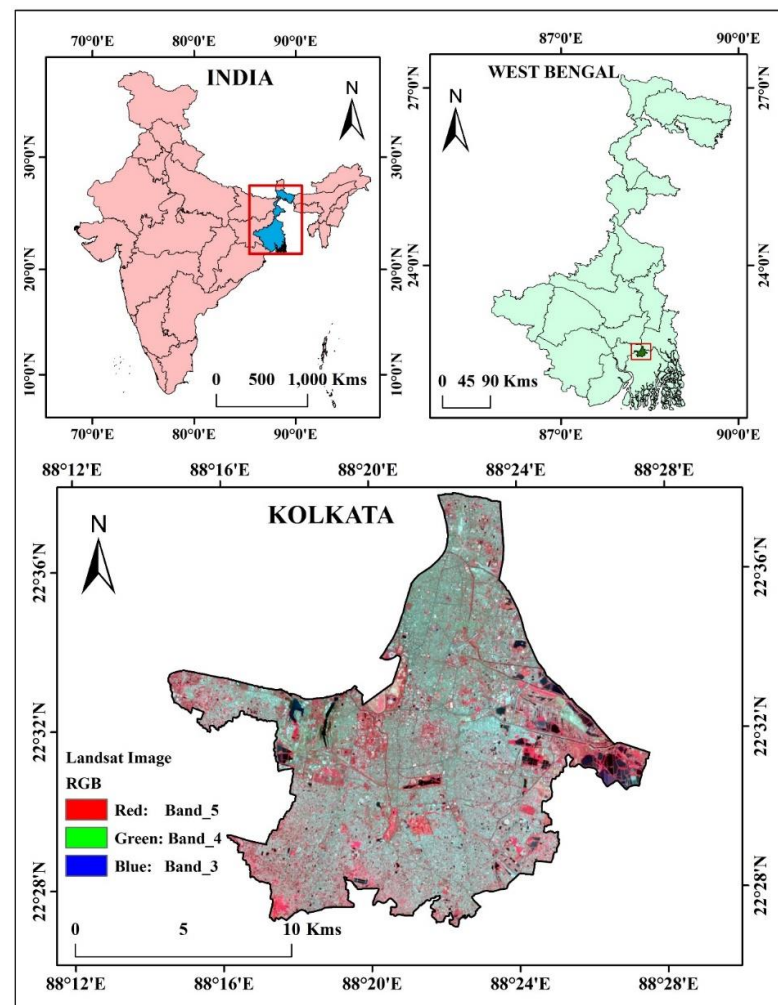


Figure 1. The location map of the case study.

2.2. Applied Datasets

The RS datasets are derived from the website USGS Earth Explorer (<https://earthexplorer.usgs.gov/>, accessed on 12 March 2023). For this analysis, six satellite datasets are used (Path 138 and row 044). The Landsat 5 TM datasets from 1991, 1996, 2001, and 2006, as well as the Landsat 8 OLI/TIRS datasets from 2016 and 2021, are used to classify the LULC of the study region and SUHI study using LST and certain spectral indicators. Table 1 is utilized for the gathering of the details of datasets (Table 1). Six satellite datasets are used in this analysis (Path 138 and row 044). Classifying the LULC of the inquiry region and SUHI study using LST and specific spectral indicators is done using Landsat 5 TM datasets from 1991, 1996, 2001, and 2006, as well as the 2016 and 2021 Landsat 8 OLI/TIRS datasets. Table 1 is used for dataset gathering and details.

Table 1. Details of satellite datasets.

Satellite	Sensor	Date of Acquisition	Path/Row	Website
Landsat 5	TM	6 March 1991	138/044	https://earthexplorer.usgs.gov/ , accessed on 12 March 2023
		20 March 1996		
		17 March 2001		
		19 June 2006		
Landsat 8	OLI/TIRS	11 April 2016		
		25 April 2021		

2.3. Image Pre-Processing and Classification

Satellite photos are initially pre-processed using RS software to perform topological, geometric, and atmospheric adjustments. ArcGIS software version 10.8 is applied for the layer stacking, masking, and ultimately the clipping of the region of interest under inspection. The human involvement in the portion of land utilized for commercial activity is known as the Land Use Change (LU). The term “Land Cover” (LC) refers to the physical features of the Earth’s surface, including vegetation, soil, water bodies, and other actual land shares [32]. The most effective approach for classifying images is through digital image processing, or DIP (Figure 2). The supervised image classification approach and a maximum likelihood algorithm are utilized for the pixel-based LULC classification. There are five classes in this examining area. Using a maximum likelihood algorithm and supervised classification technique, vegetation, built-up land, bare land, and grassland are classified (Table 2).

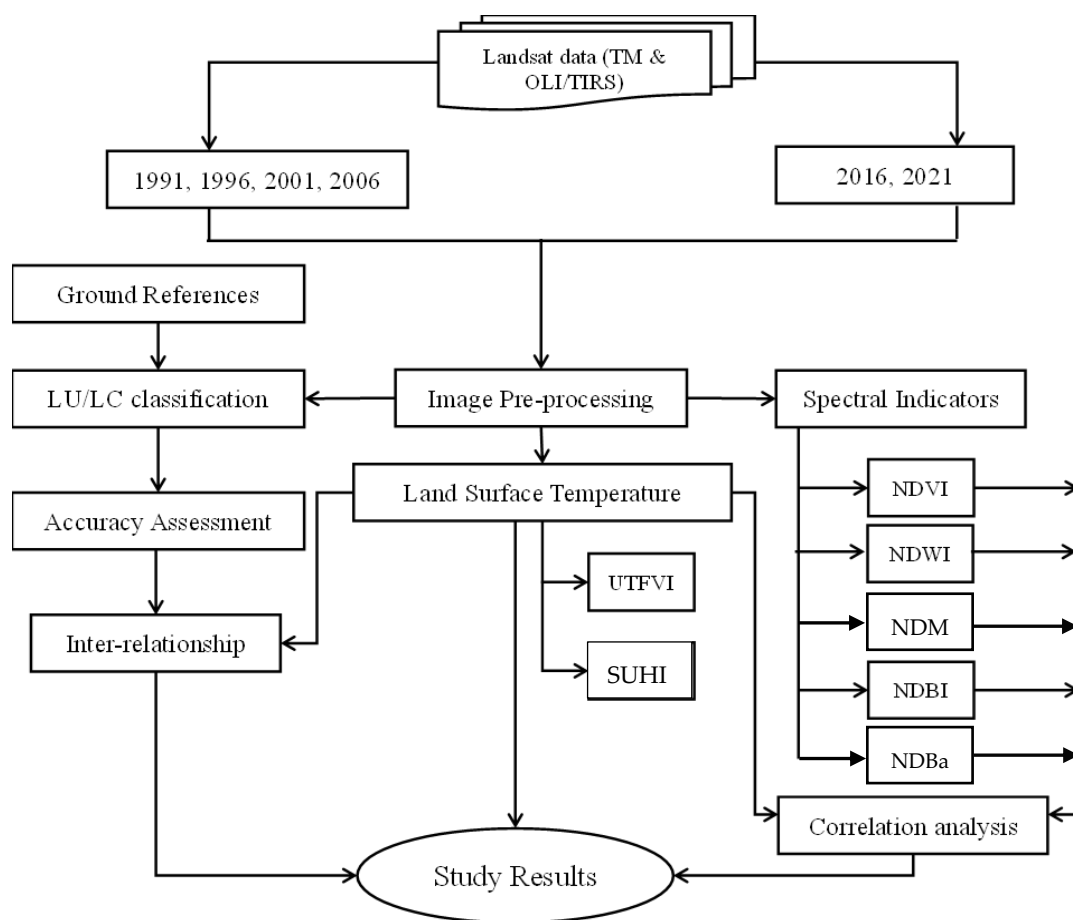


Figure 2. The modelling framework of the adopted methodology.

Table 2. LULC classes applied in this study classification.

Built-up land	Residential area, commercial area, industrial area, transportation, roads, and construction area.
Vegetation	Evergreen forest, deciduous Forest Land, Mixed Forest Land, Shrub/degraded vegetation.
Water Bodies	River, Ponds, lakes, and open water bodies.
Bare land	These types of classes are mainly playgrounds, open area, and many others.
Grass Land	Many types of trees, Grass area, open vegetated area

2.4. Accuracy Assessment and Kappa Statistic

Accuracy assessment comes in the post-classification stage. The urban areas consist of a diverse range of features, such as residential areas, water bodies, roadways, green spaces, and railroads [33]. Since this approach indicates the correctness of the classification outcomes, the accuracy assessment has the biggest important influence after the classification [34]. This method is used to associate both categorized and ground truth datasets. Google Earth Pro and field surveys make up the ground truth datasets. The accuracy of classification is assessed using the Non-parametric Kappa test. In addition to being a diagonal element, the Kappa coefficient also forms the basis of the misperception matrix [34]. Following this equation is the calculation of the Kappa coefficient (Table 3).

$$k = \frac{N \sum_{i=1}^r X_{ii} - \sum_{i=1}^r (X_{i+} X_{+i})}{N^2 - \sum_{i=1}^r (X_{i+} X_{+i})} \quad (1)$$

Table 3. The scale of Kappa coefficient.

SL. No	Value of K	Strength of Agreement
1	<0.20	Poor
2	0.21–0.40	Fair
3	0.41–0.60	Moderate
4	0.61–0.80	Good
5	0.81–1.00	Very Good

2.5. Geo-Spatial Indices

2.5.1. NDVI

Green space was the most significant feature of Earth's surface because it regulates temperature swings, surface runoff, infiltration rate, soil erosion losses, drought control, and water level over the land's surface [35,36]. Many areas were losing their green space land due to urbanization, which also caused droughts, temperature fluctuations, and increased evapotranspiration [6,37]. The land transformation also influenced the green space situation. The monitoring of the vegetation state made considerable use of the Landsat 5 TM and 8 OLI/TIRS datasets [38,39]. The NDVI, which can be expressed by applying Equation (2), was used in the current investigation to assess the health status of green spaces in Kolkata, West Bengal.

$$NDVI = \frac{(\rho_{NIR} - \rho_R)}{(\rho_{NIR} + \rho_R)} \quad (2)$$

where R represents the red band of satellite datasets and NIR indicates the near-infrared band of the Landsat imageries. The remaining LULC classifications are denoted by 0 to -1 in the $NDVI$ standards, while a region's healthy green space is indicated by 0 to $+1$.

2.5.2. NDBI

Urban growth affects environmental deprivation and localized climatic change [40,41]. In the megacity of Kolkata, population density has a significant impact on both urban development and the expansion of built-up territory. Urban planning is more important for sustainable urban growth, although conditions are eliminated by excessive population density [42,43]. The megacity of Kolkata has seen significant infrastructure growth in the past. Such urban expansion was observed using the $NDBI$.

$$NDBI = \frac{(\rho_{SWIR1} - \rho_{NIR})}{(\rho_{SWIR1} + \rho_{NIR})} \quad (3)$$

In satellite imagery collections, the acronym *SWIR* refers to shortwave infrared bands, while *NIR* denotes near-infrared bands. The *NDBI* guidelines range from -1 to $+1$. Positive standards are built-up areas, while negative standards represent other LULC traits.

2.5.3. NDMI

Urbanization generally lowers relative humidity (RH) because of the higher temperatures and less surface water that can evaporate, in addition to aggregating the temperature over the megacity. The Landsat TM, ETM+, and OLI/TIRS near-infrared (NIR) and short-wave infrared bands were used to calculate the NDMI (<https://www.usgs.gov/core-science-systems/nli/landsat/normalized-difference-moisture-index>, accessed on 12 March 2023). The NDMI can be determined by using Equation (4).

$$NDMI = \frac{(\rho_{NIR} - \rho_{SWIR1})}{(\rho_{NIR} + \rho_{SWIR1})} \quad (4)$$

The areas with problems with water stress will be categorized using the normalized differential moisture index standards. Typically, the *NDMI* norms fall between -1 and 1 .

2.5.4. NDBaI

The normalized difference bareness index is typically used to determine the exterior hardness of the infertile ground. Applying the *SWIR* and thermal infrared (*TIR*) bands as forecasted by Zhao and Chen yields the *NDBaI* [44].

$$NDBaI = \frac{(\rho_{SWIR1} - \rho_{TIR})}{(\rho_{SWIR1} + \rho_{TIR})} \quad (5)$$

2.5.5. NDWI

With the NDWI applied to satellite imagery, open water landscapes were brought to light, making a body of water “pop out” in contrast to the surrounding soil and vegetation [45].

$$NDWI = \frac{(\rho_G - \rho_{NIR})}{(\rho_G + \rho_{NIR})} \quad (6)$$

2.6. LST Estimation

The thermal difference and the heat change of a region are prejudiced by the LST [46]. The megacity of Kolkata’s land surface temperature (LST) is monitored using the Landsat 5 TM (Band 6) and the Landsat 8 OLI/TIRS (Band 10). To monitor the LST, data from Landsat OLI/TIRS for 2016 and 2021, as well as Landsat TM datasets for 1991, 1996, 2001, and 2006, are used. Landsat 8 has two thermal bands, namely 10 and 11. But band 11 was not treated in this evaluation because of the possibility that it will rise in the LST approximation due to the satellite orbit’s tilt. As a result, only the Landsat band 10 is used to approximate the LST imagery in the megacity of Kolkata. Las Vegas and Baghdad are two different cities in the world whose temperature changes are calculated using the LST of four decadal Earth observation datasets. The land surface temperature (Band 10) is designed using Landsat TM (Band 6) and Landsat OLI/TIRS [47]. The process that follows is utilized to advance the LST maps of certain research areas [48]. Thermal fluctuation is greater in urban areas than in rural ones. The metropolitan areas that are green or blue have a lower temperature than the surrounding areas. In the area under research, the location and effect of temperature are displayed by the LST charge. The complete computing process for Landsat 5 and 8 LST is defined in the literature. The SUHI remained resolute through the LST. A shift in surface temperature was connected to a modification in LULC. Regular updates are made to the SUHI requirements.

2.7. UTFVI

The SUHI's effects were often described using the UTFVI. The SUHI and UTFVI singularities are the result of several factors influencing land surface temperature, psychometrics, and light intensity, such as heat waves and Earth surface modification [49]. The formula below was used to determine the UTFVI.

$$UTFVI = \left(\frac{T_s + T_{mean}}{T_{mean}} \right) \quad (7)$$

where T_s signifies the LST in kelvin, and T_{mean} is used to display the mean LST in kelvin. The UTFVI is categorized into six groups according to the reflected changes in the urban thermal field: none, moderate, intermediate, strong, stronger, and strongest.

2.8. SUHI

The investigation of SUHI is significant for the study of urban heat balance. The SUHI diagram is projected to regulate the heat variation in the Kolkata megacity area:

$$SUHI = \left(\frac{T_s + T_{mean}}{SD} \right) \quad (8)$$

where T_s stands for the LST (K), T mean is the mean LST (K), and SD is the standard deviation of the estimated LST map.

3. Results and Discussion

The three-colour bands' composition (blue, green, and red) is applied for classification based on six altered years of the Landsat 5 TM and Landsat 8 OLI/TIRS datasets. Between KMC and environs regions, there has been a foremost LULC change in the aforementioned 30 years as an outcome of urban growth. At large, population growth is controlled, but the built-up region is quickly improved, while water bodies, vegetation, and grassland are deceptively reduced in maximum portions of the investigation region. The diminuendos of LULCC are predictable from the year 1991 to 2021. The outcomes will be deliberated in the subsequent subdivisions.

3.1. Areal Change of LULC

The supervised classification technique with a maximum likelihood algorithm is utilized to recognize the LULCC outlines from the year 1991 to 2021. Five categories of LULC are identified in LULC diagrams: built-up land, grassland, bare ground, vegetation, and aquatic bodies. Due to the disastrous process of urbanization and population increase, the entire region has displayed a water body, a decline in vegetation, bare ground, and grassland. The percentages of the vegetation region are acknowledged as 21.82% (1991), 35.52% (1996), 7.40% (2001), 15.62% (2006), 26.07% (2016), and 14.52% (2021), correspondingly (Table 4), over the investigation zone. The water body variations regions over the years were 875.43 Ha (1991), 614.43 Ha (1996), 523.89 Ha (2001), 682.56 Ha (2006), 785.97 Ha (2016), and 441.27 Ha (2021), correspondingly. Due to the urbanization of such areas, a 434.16 Ha water body region has shrunk throughout the last 30 years (Figure 3). According to the land modification examination, many vegetated lands have changed into various LULC features that can be experienced in terms of infiltration rate, soil moisture content, and slope stability. The residential zone close to the industrial region has significantly intensified in the KMC area. High temperatures and air pollution consistently plagued the populated zones, and the SUHI result was also observed in this location (Table 4). The grassland has shown a reduction from 27.63% (1991) to 22.63% (1996), 31.95% (2001), 29.97% (2006), 9.13% (2016), and 15.31% (2021), and a total grassland of 2286.9 Ha has been reduced in the past 30 years (Figure 4). The classified diagrams show enormous variations in the built-up lands, which enlarged from 41.61% (1991) to 37.60% (1996), 55.19% (2001), 50.69% (2006), 54.27% (2016), and 67.10% (2021), respectively (Table 5). Along with lowering the

temperature, these built-up locations have also significantly lowered the rate of infiltration and surface runoff escalation.

Table 4. Area calculation of the different years' classification.

Class Name	Area in Ha					
	1991	1996	2001	2006	2016	2021
Water body	875.43	614.43	523.89	682.56	785.97	441.27
Vegetation	4050.27	6591.51	1374.03	2899.44	4837.77	2695.41
Grass Land	5127.93	4198.95	5928.21	5561.55	1694.25	2841.03
Built-up Land	7721.55	6978.15	10,241.73	9406.98	10071	12,450.78
Bare Land	779.04	171.18	486.36	3.69	1165.23	125.73

Class Name	Area in Percentage (%)					
	1991	1996	2001	2006	2016	2021
Water body	4.71	3.31	2.82	3.67	4.23	2.37
Vegetation	21.82	35.52	7.4	15.62	26.07	14.52
Grass Land	27.63	22.63	31.95	29.97	9.13	15.31
Built-up Land	41.61	37.6	55.19	50.69	54.27	67.1
Bare Land	4.19	0.92	2.62	0.01	6.28	0.67

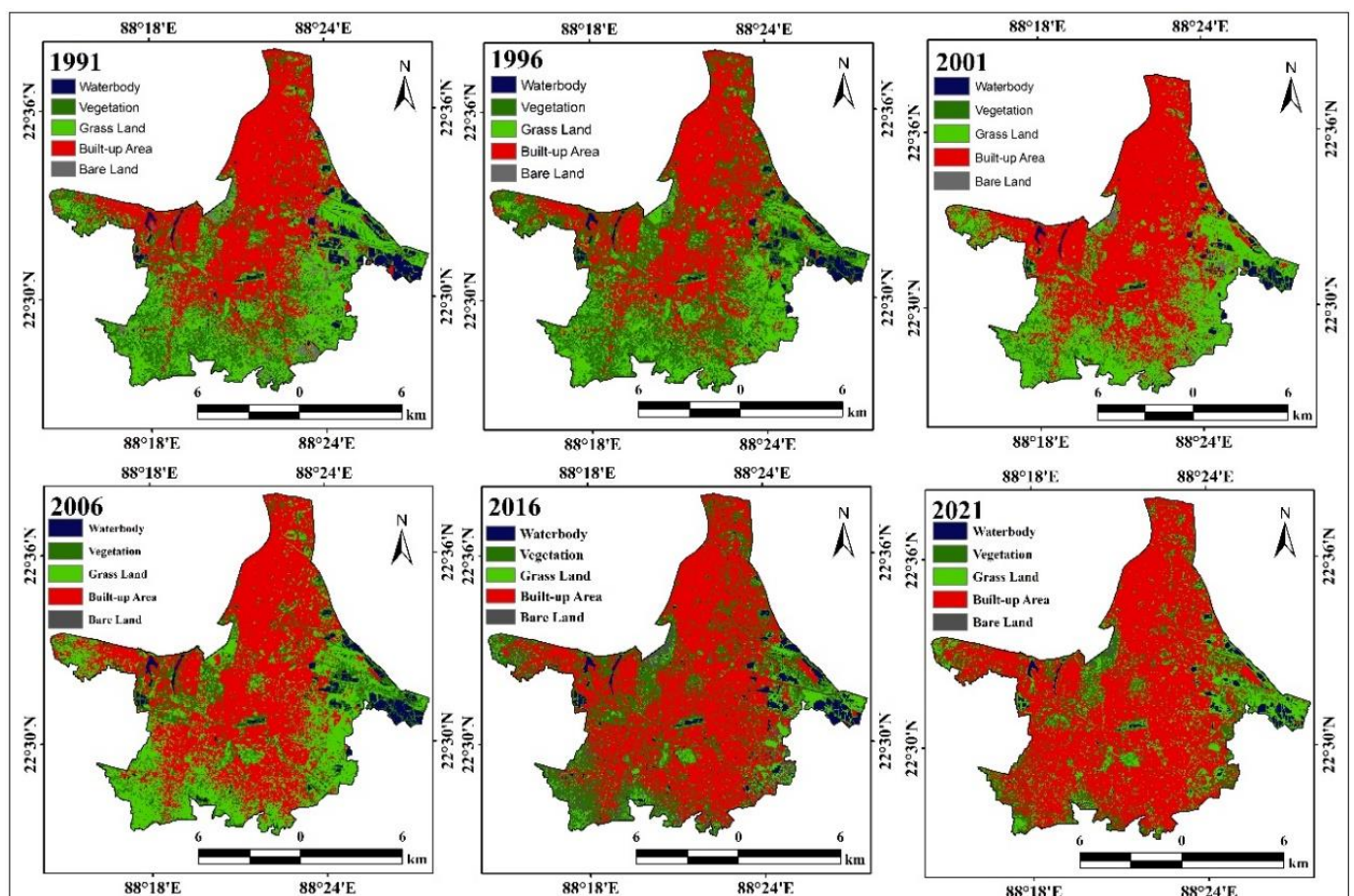


Figure 3. Maps of the land cover/use of the studied Kolkata district.

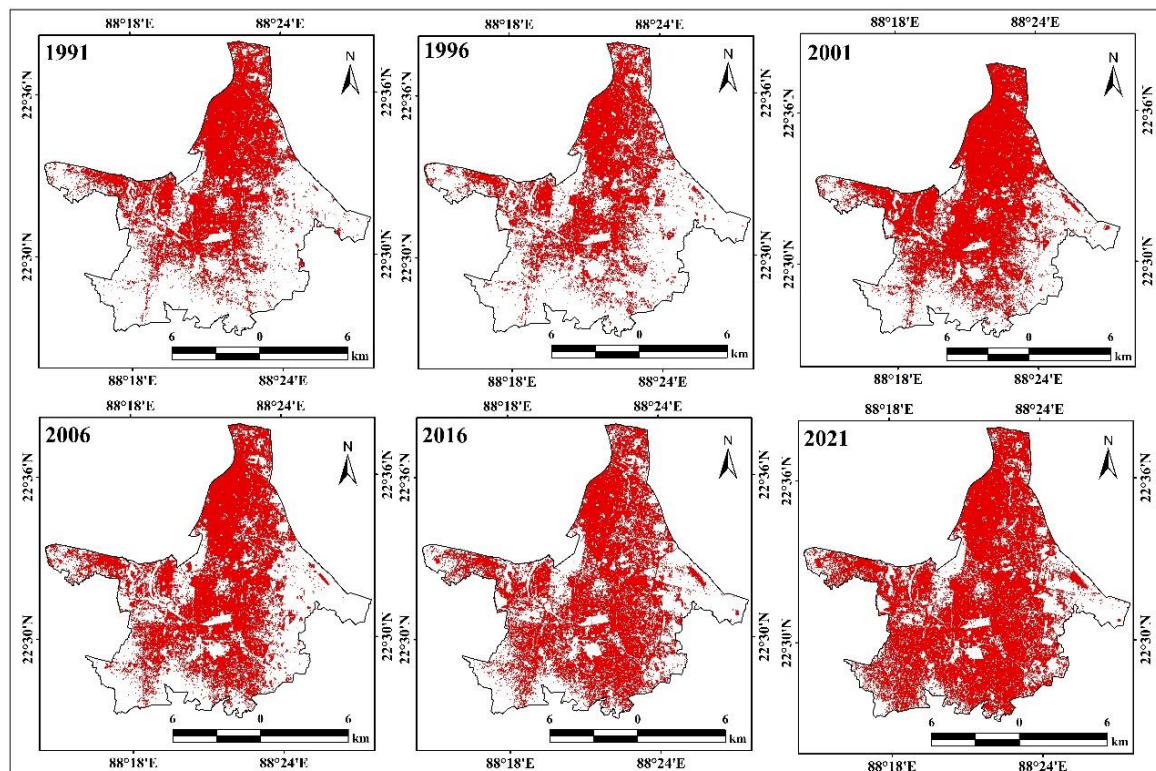


Figure 4. Maps of built-up land in different years (1991–2021).

Table 5. Loss/Gain analysis of different periods.

Class Name	Area Increased/Decreased (Ha)					
	(1991–1996)	(1996–2001)	(2001–2006)	(2006–2016)	(2016–2021)	(1991–2021)
Water body	−261	−90.54	158.67	103.41	−344.7	−434.16
Vegetation	2541.24	−5217.48	1525.41	1938.33	−2142.36	−1354.86
Grass Land	−928.98	1729.26	−366.66	−3867.3	1146.78	−2286.9
Built-up Land	−743.4	3263.58	−834.75	664.02	2379.78	4729.23
Bare Land	−607.86	315.18	−482.67	1161.54	−1039.5	−653.31

Notwithstanding the LULC elements listed above, the remaining LULC elements also share a striking amount of dynamic similarity. Bare land (0.55), built-up (0.52), and fallow land (0.56) dynamicity are close to each other in agricultural land dynamics. It is discovered that homestead dynamics with a plantation are almost identical to those of bare land (0.53). The similarity index values of 0.53 and 0.57, respectively, indicate that the dynamics of built-up areas are nearly identical to those of homesteads with plantations and water bodies [50]. Over the previous 20 years, there has been a 108.94 km² spatial growth due to the growing urban population. Moreover, 88.71 km² in 1989, 144.64 km² in 2006, and 197.65 km² in 2010 make up the urban built-up area within and surrounding the city. These modifications have raised the study region's surface temperature. Biophysical parameter analysis reveals a negative association between NDBI and NDWI, a negative correlation between LST and NDVI, and a positive correlation between LST and NDBI [51]. Urban built-up, open terrain, vegetation, agricultural land, and aquatic bodies are the five classes into which the multi-temporal satellite data are classified using the supervised Maximum Likelihood Classification technique. The findings showed that new road construction, flyovers, settlement building, etc., caused the urban built-up area to gradually rise by roughly 21.17% (239.097 km²) throughout the study period. Other geographical features have gradually decreased, including open space, flora, agricultural land, and bodies of water [52].

A built-up zone was developed on 4729.23 hectares of natural land after the categorized LULCC diagrams from 1991 to 2021 were examined. The differences in the bare land zone are recorded as 4.19% (1991), 0.92% (1996), 2.62% (2001), 0.01% (2006), 6.28% (2016), and 0.67% (2021), and a total decrement of 653.31 Ha (1991–2021) of bare land is detected above the investigation regions (Figure 5). The overall accuracy assessment outcomes for LULC classification are 93% (1991), 95.59% (1996), 92.97% (2016), and 92.94% (2021), respectively. Apart from that, the kappa statistics for the years 1991, 1996, 2016, and 2021 are obtained, respectively, and they are 0.91, 0.94, 0.91, and 0.91. Large-scale land changes in Kolkata's megacity have intentionally impacted the local ecology and natural environmental conditions (Figure 6). The vegetation decrease and high thermal variation have increased the SUHI effects in the investigation region [53].

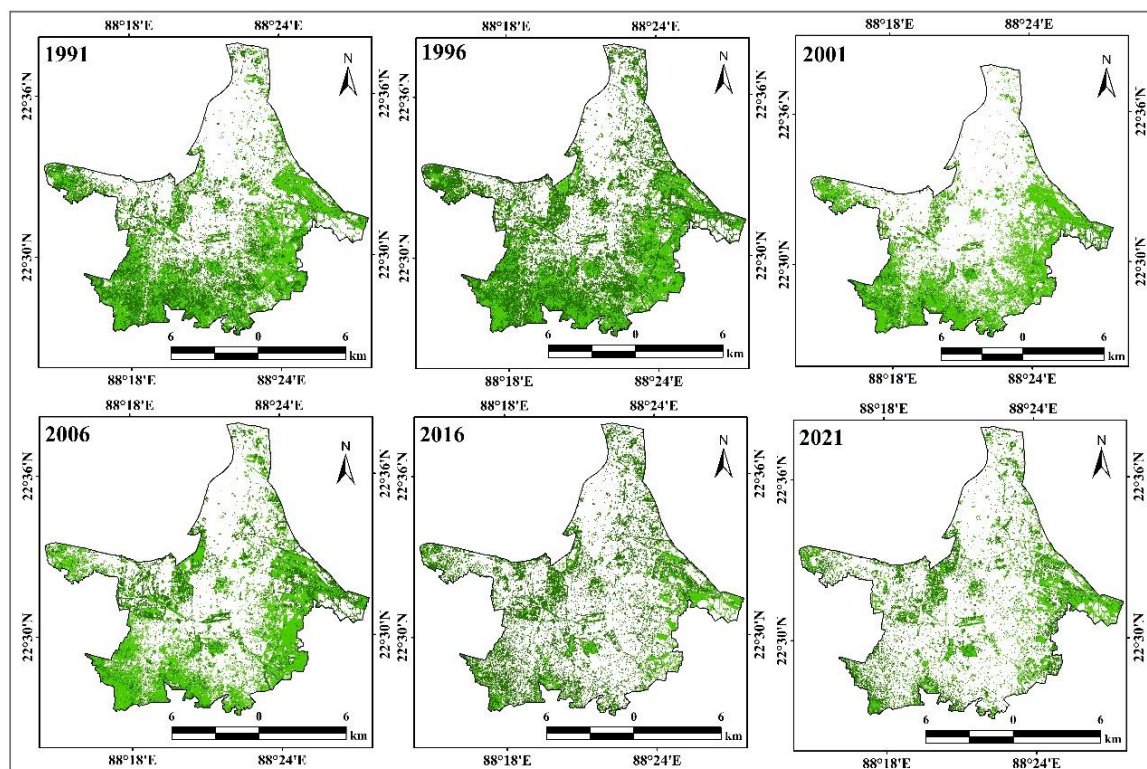


Figure 5. Maps of vegetation land in different years (1991–2021).

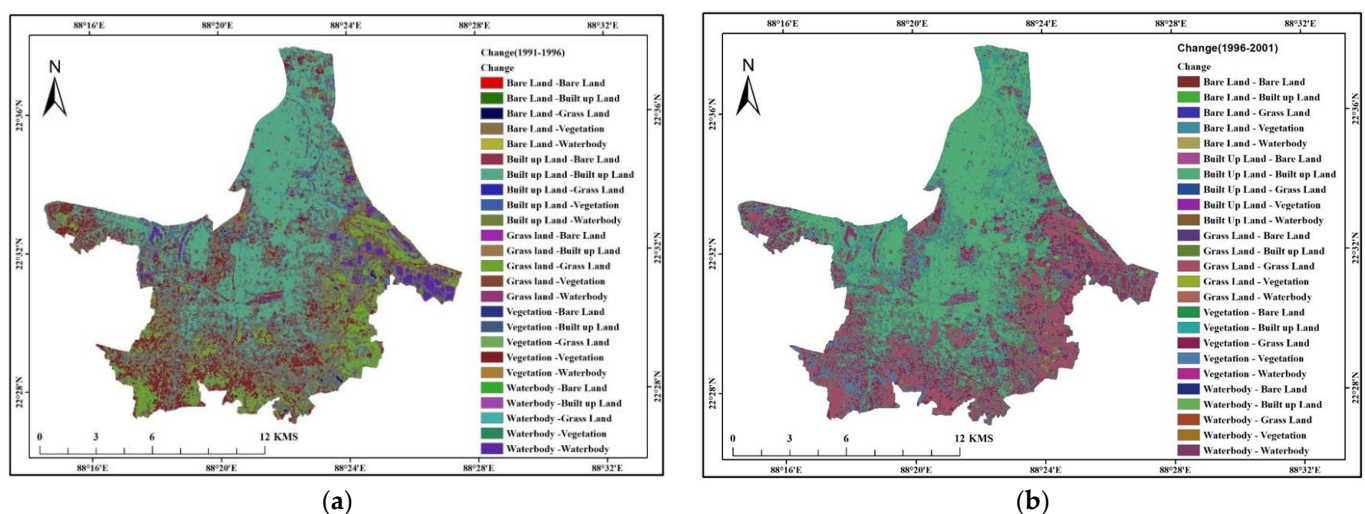


Figure 6. Cont.

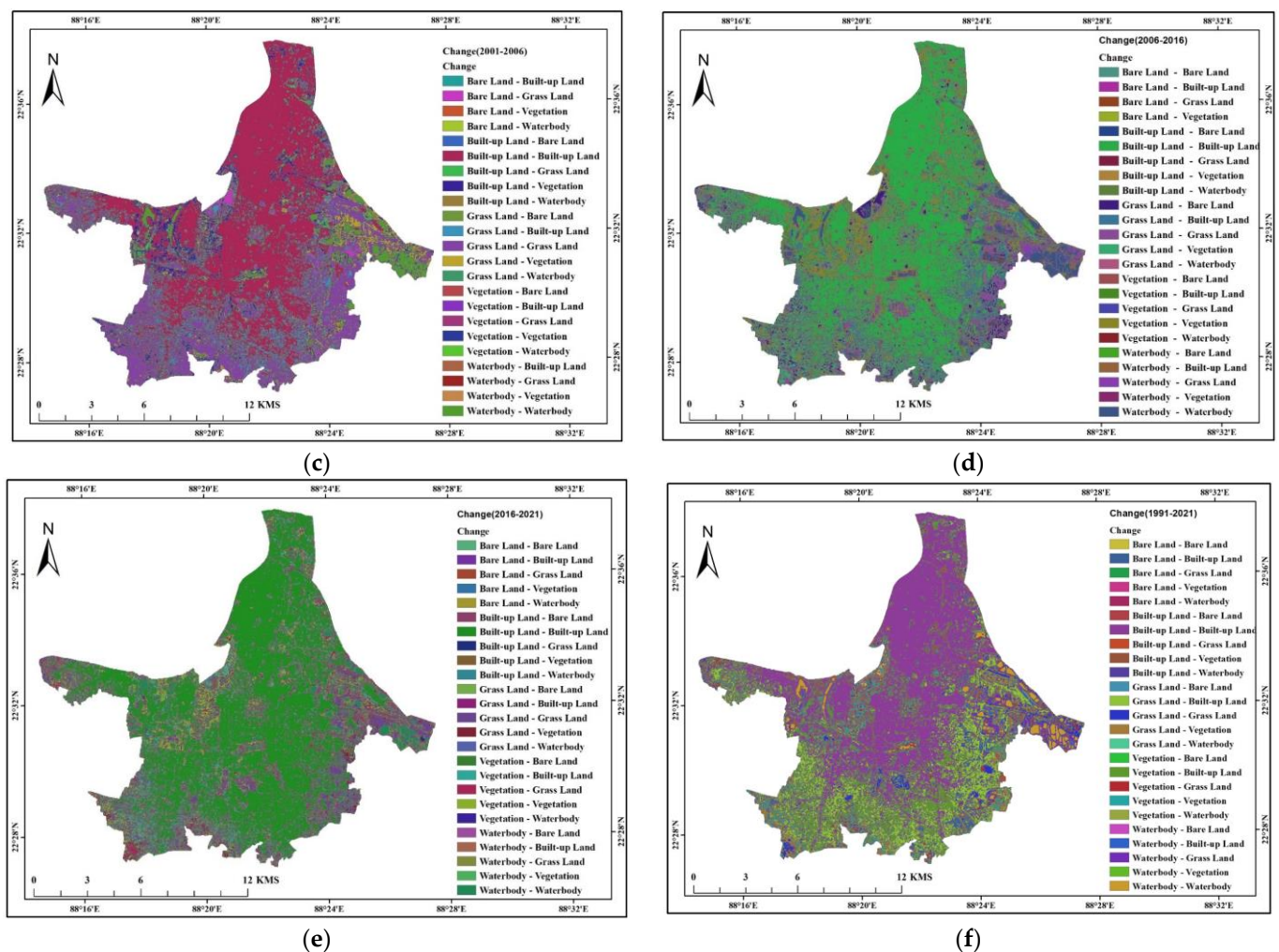


Figure 6. Change detection of LULC (a) 1991–1996; (b) 1996–2001; (c) 2001–2006; (d) 2006–2016; (e) 2016–2021; (f) 1991–2021.

3.2. LST Variation

This area experienced wide variations in temperature in different areas due to the growth of the cities. Due to human activity, the center sections are situated in areas with significant temperature variations. Verifications of the Earth's surface temperature variations and high points throughout 1991–2021 correspond with the spatial circulation of the regions under examination. In various areas of the research site, open space and grasslands are converted into developed areas. The temperature in any given area determines the type of vegetation. The application of the known equation to remote sensing (RS) data from Landsat 5 TM and 8 OLI thermal bands produced the spatio-temporal disseminations of land surface temperature (LST) for the years 1991–2021. This diagram's red hue indicated the highest temperature, while the blue colour indicated the lowest temperature in real-time (Figure 7). The LST varies in the following years: 1991, 20.62 °C to 30.83 °C with a mean temperature of 25.72 °C; 1996, 22.97 °C to 31.26 °C with a mean temperature of 27.11 °C; 2001, 23.94 °C to 32.05 °C with a mean temperature of 27.99 °C; 2006, 23.97 °C to 33.05 °C with a mean temperature of 27.995 °C; 2016, 24.67 °C to 35.59 °C with a mean temperature of 30.13 °C; and 2021, 25.32 °C to 38.82 °C with a corresponding mean temperature of 32.07 °C. The annual differences in the hottest and lowest temperatures between 1991 and 2021 are around 5.81 °C and 7.72 °C, respectively. The annual temperature rose every year between 1995 and 2020, and there was a notable rise in the mean land surface temperature (LST) due to the conversion of agricultural land and trees outside forests (TOF) to built-up areas. Compared to the suburbs, the mean LST over Kolkata City was rather high.

The average land surface temperature (LST) increased by 4.32 °C in the winter and by approximately 8.43 °C in the summer between 1995 and 2020. Over built-up areas (7.06 °C), agricultural land without crops (5.55 °C), and open land (5.54 °C), the rate of increase in LST was found to be relatively high. Over TOF (4.66 °C) and water bodies, however, it was quite low (3.68 °C) [54].

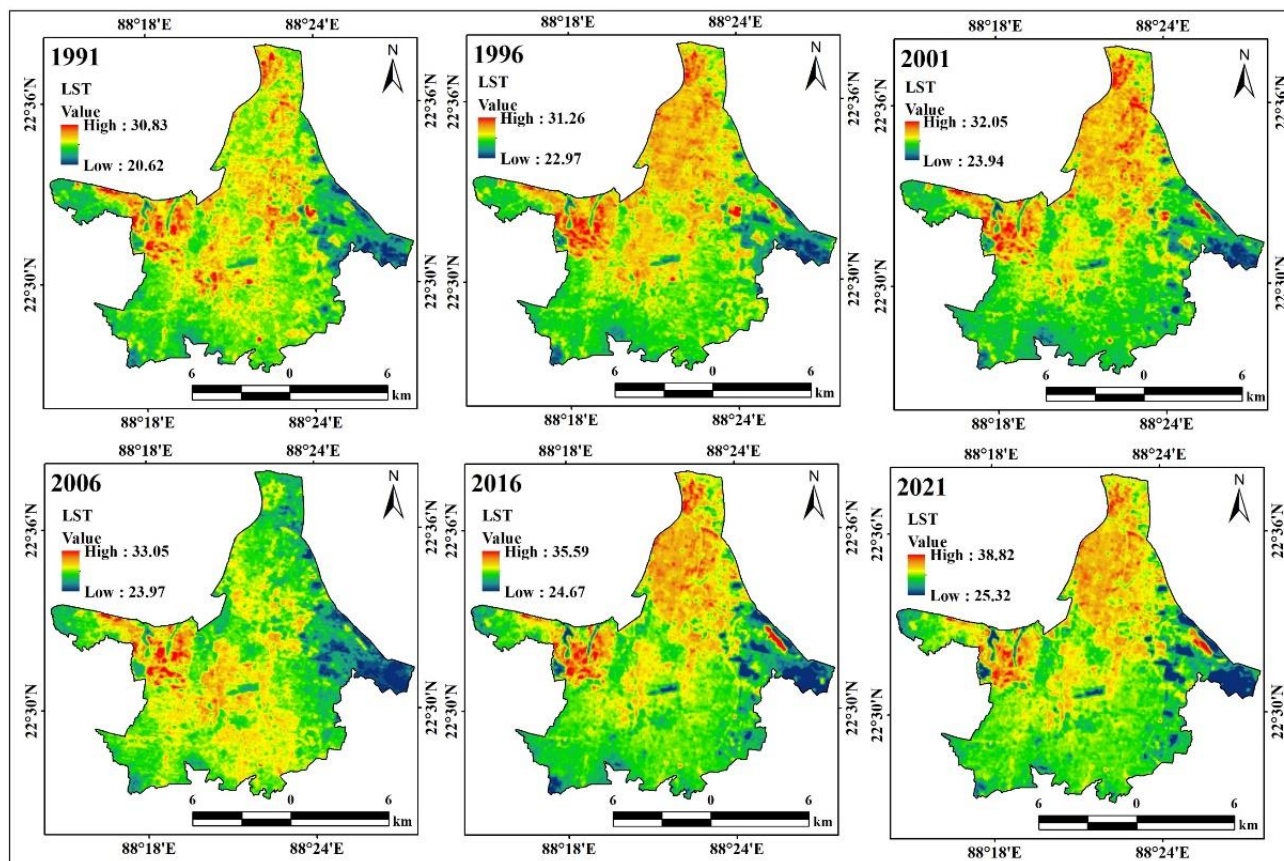


Figure 7. Maps of the LST in different years (1991–2021).

3.3. Geo-Spatial Indices

The SUHI study is classified using RS-based dissimilar spectral indices. The NDWI, NDBI, NDMI, NDVI, and NDBal are computed using the Landsat 5 TM and Landsat 8 OLI/TIRS bands (NDBal). The urban zone grew over the years, according to the NDBI graphic. The primary cause of the devastating fall in heat differential is likewise the decline in the vegetated zone in such zones. This inquiry region's altered flora is depicted in the NDVI graphic. Many areas of this region had a healthy green space in 1991; however, those areas were aware of the degradation of the green space due to population pressure and urbanization. Because there are differences in land values in different areas of the region under examination, the urban area has grown. The land value in KMC and its surrounding areas is generally high, while there are occasional times of low land value in other places. As a result, the societies were able to relocate to the nearby KMC and benefit from the development and convenience of the Kolkata metropolitan area. The south, west, and northeast regions of this study area have had substantial changes to the green space during the past 20 years, according to the NDVI diagram of various years. The locations of Rajarhat-Newtown, Khidirpur, Amta, Sonarpur-Rajpur municipality, and Pujali have reduced the amount of green space. The SUHI influence on the area under investigation is also produced via the Urban Thermal Field Variance Index (UTFVI) figure. Urban expansion is causing a significant rate of value alteration in the RS technique-based UTFVI. There were also significant thermal field variations between 1991 and 2021 in

the areas surrounding Khidirpur, Kolkata port, Dharmotola, Sealdha station, and Netaji Subhash Chandra Bose International Airport. Urbanization caused a 0.015 Urban Thermal Field Variance to increase everywhere throughout those years. This study highlights how urbanization has significantly impacted the area under investigation and shows a persistent pattern of green space conversion into built-up areas during the investigation. As a result of this change, there is less greenery and a rise in surface temperatures. Via NDVI, NDBI, and LST studies, this study shows strong relationships and patterns, highlighting the necessity for urban planners, environmentalists, and ecologists to give this issue their full attention [55]. The regulatory amplitudes for the NDBI and albedo were highest because the marginal effect values had the biggest range. When the BCR changed from 0.3 to roughly 0.5, there was an increase in the positive link between NDBI and BCR and LST. When it was more than 60%, there was a substantial negative correlation between GS and LST. There was some complexity in the correlations between LST, SVF, and NDVI, respectively. When the NDVI values were greater than 0.6, the relationship between the NDVI and LST turned negative. Otherwise, there was a generally positive correlation between the two variables. After surpassing 0.8, the connection between SVF and LST turned positive. Between 0.2 and 0.8, it was negative [56].

To control the area of vegetation deterioration between 1991 and 2021, the NDVI was computed (Figure 8). Due to the region under study's ongoing urbanization and deforestation, the NDVI interpretations based on the various years demonstrated a significant reduction in the green space region. The NDVI's experiential interpretations from 1991 are 0.63 and -0.34 , respectively, representing the highest and lowest interpretations. However, the NDVI interpretations have reduced unexpectedly with the maximum value individually validated as 0.44, while the lowest reading is -0.10 . Because there is less greenery or grassland over KMC regions, the NDVI values in urban and industrial zones are often low. the years 1991 to 2021. Everywhere 0.015 Urban Thermal Field Variance amplified throughout those years due to urbanization.

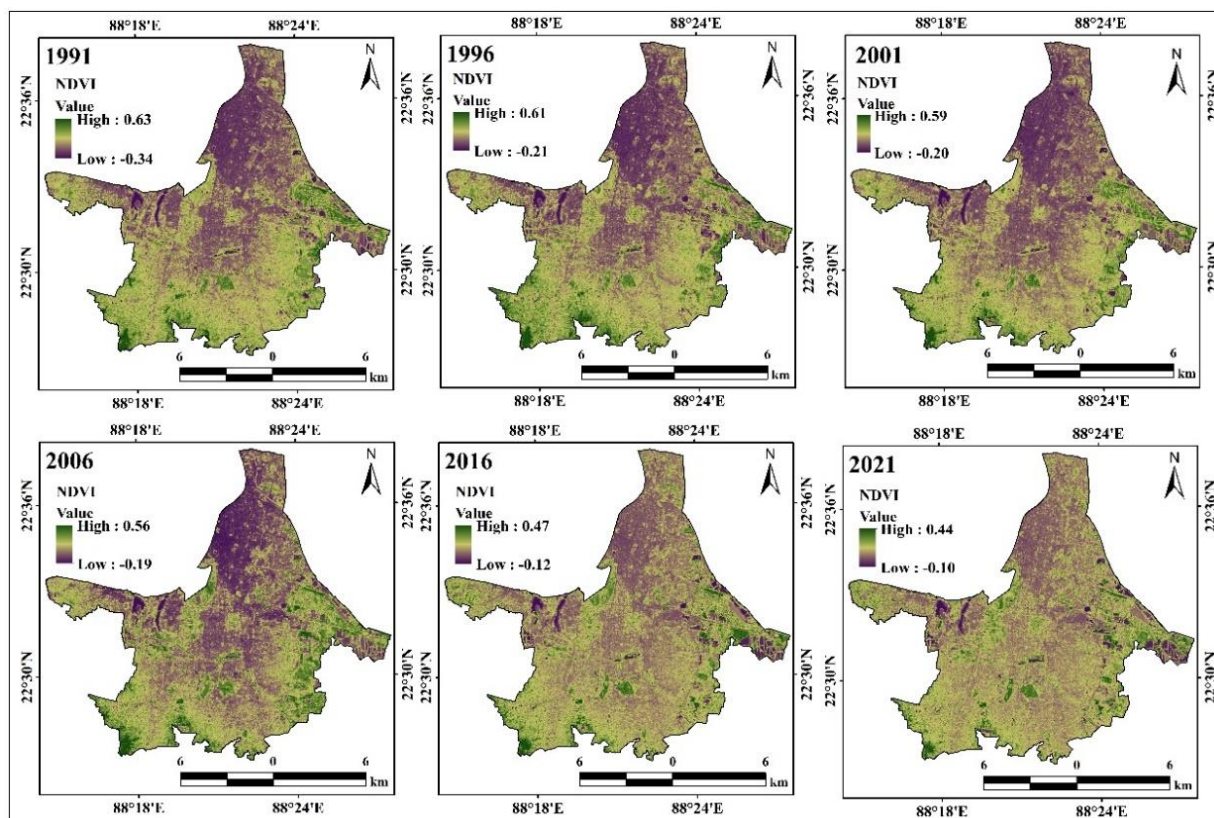


Figure 8. Maps of the NDVI in different years (1991–2021).

Satellite imagery was used to track this metropolitan megacity's built-up expansion over several years. To compute the built-up indicators for six distinct years, two bands were used. According to the NDBI results, over the last 30 years, the greatest significance rose from 0.38 (1991) to 0.49 (2021). This discovery indicates that the examined region's built-up land and urban expansion became appealing locations quickly (Figure 9). The NDMI scale runs from -1 to $+1$, with the lowest requirements representing low water content in green spaces and the highest criteria representing high water content. Stated differently, a decrease in the NDMI will be indicative of water stress, whereas abnormally high NDMI values may suggest waterlogging. The NDMI's high requirements are 0.62 (1991), 0.52 (1996), 0.48 (2001), 0.40 (2006), 0.35 (2016), and 0.32 (2021). In some areas of the region under examination, the NDMI's standards have decreased. Over the last 30 years, the overall NDMI norm of 0.3 has been lowered (Figure 10). The entire inspecting area's bareness level is categorized using the bareness index. The maximum standards varied between 0.17 (1991) and 0.08 (2021), continually. The substantial built-up growth over the examination zone caused the NDBal to be gradually reduced in the same manner (Figure 11). The high standards of NDWI are 0.38 (1991), 0.23 (1996), 0.21 (2001), 0.20 (2006), 0.13 (2016), and 0.12 (2021). The NDWI standards reduced in certain portions of this examining region. A total NDWI standard of 0.18 has been condensed in the past 30 years (Figure 12).

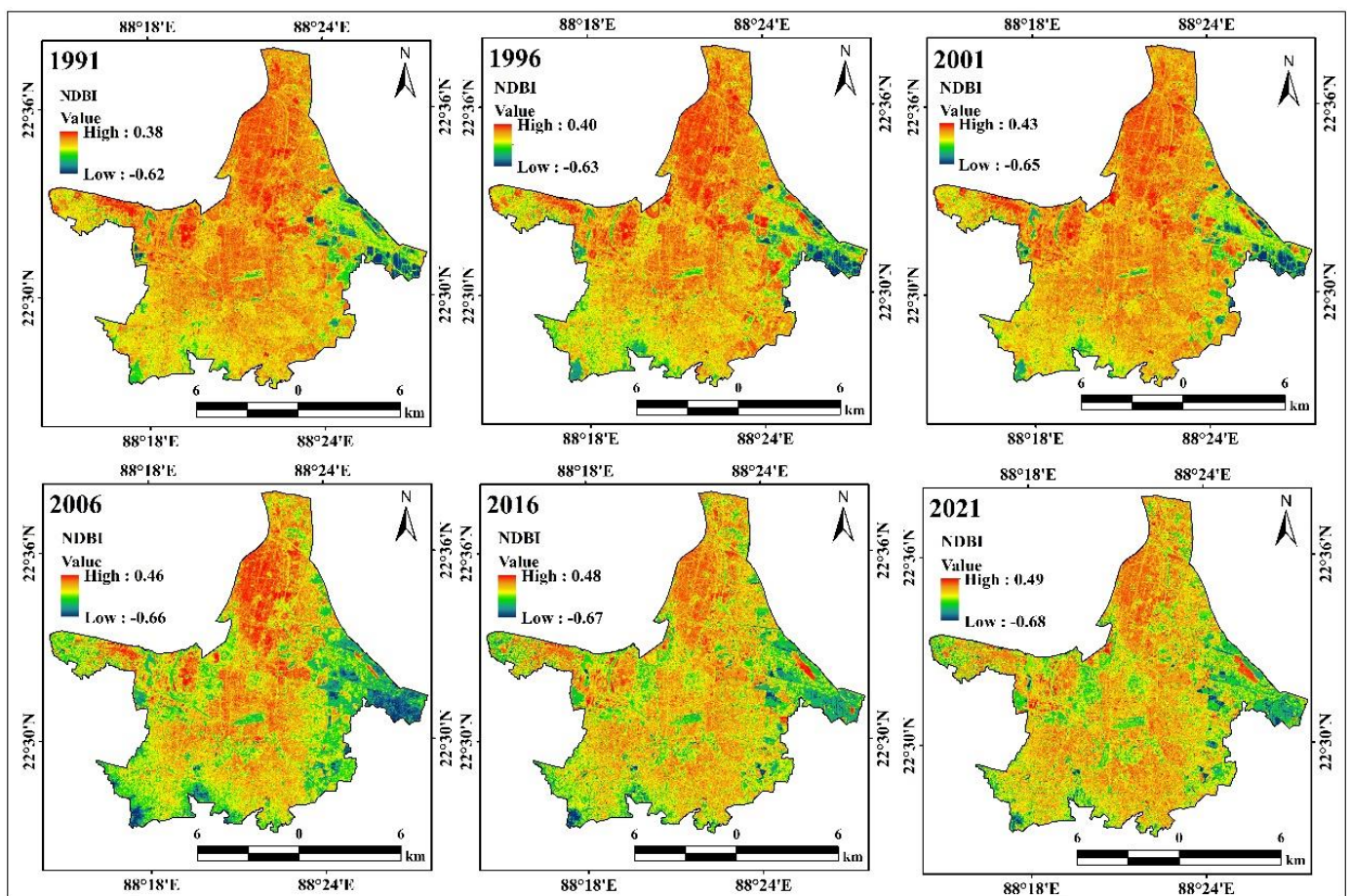


Figure 9. Maps of the NDBI in different years (1991–2021).

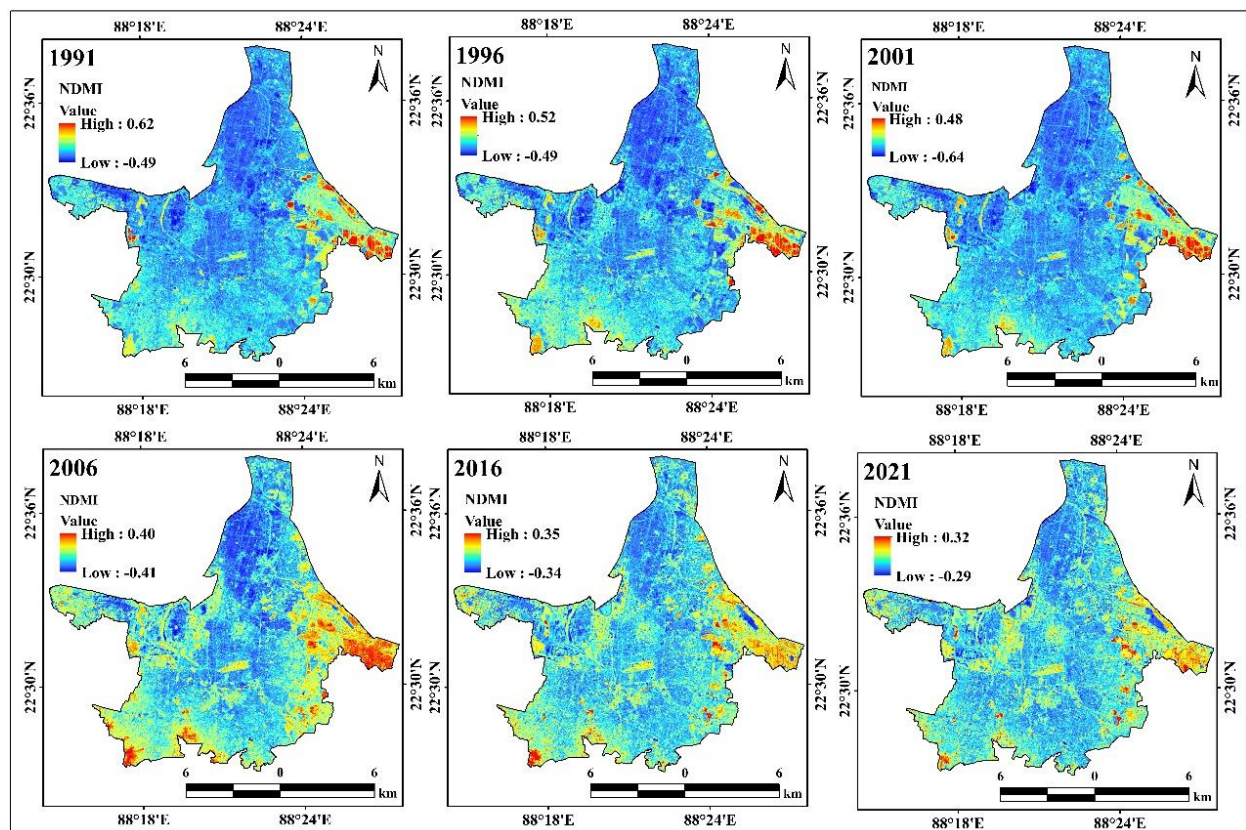


Figure 10. Maps of the NDMI in different years (1991–2021).

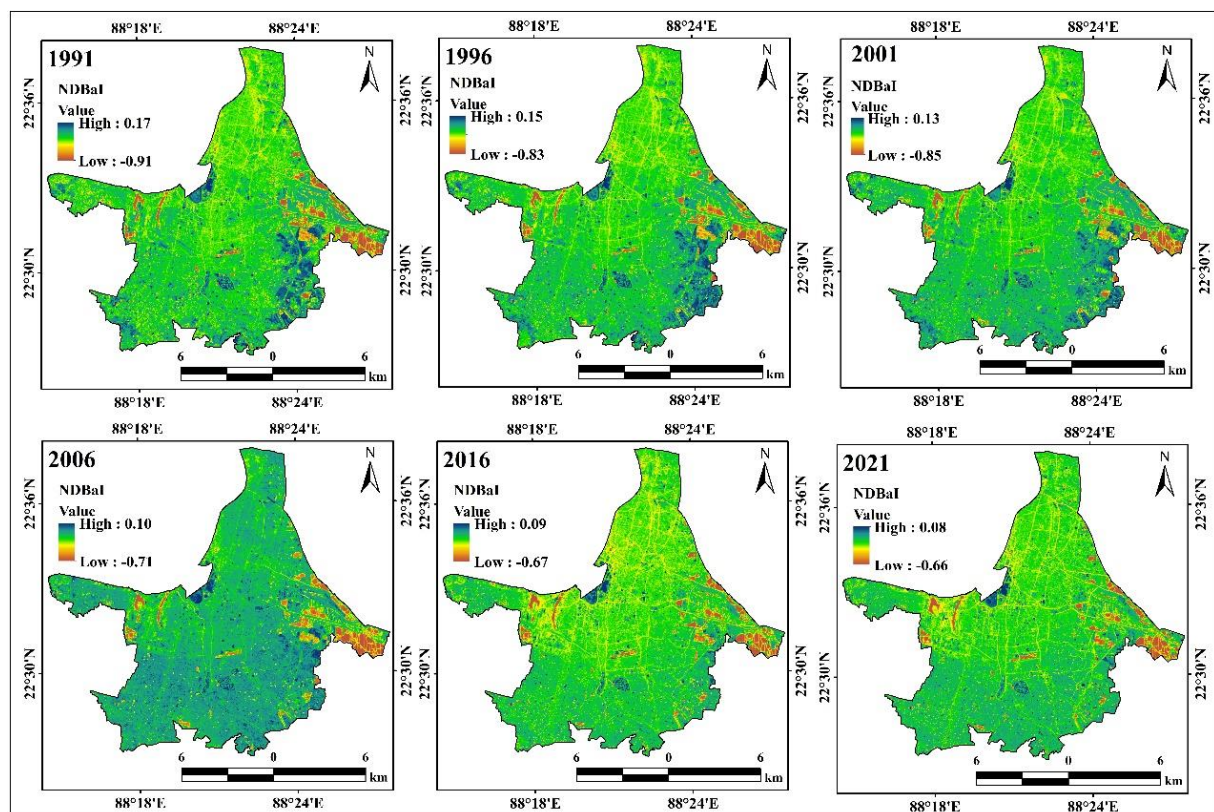


Figure 11. Maps of the NDBaI in different years (1991–2021).

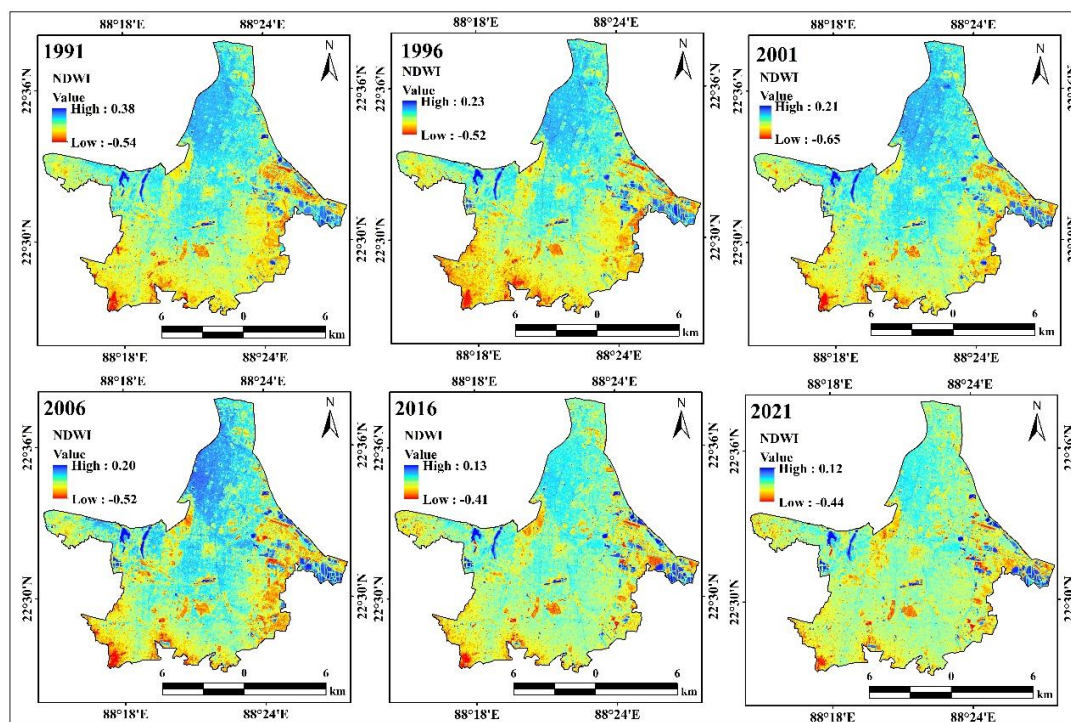


Figure 12. Maps of the NDWI in different years (1991–2021).

3.4. SUHI

The SUHI calculation is additionally significant for environmental situation supervision and preparation for a better future (Figure 13). In every corner of the world, people migrated in the direction of the cities. In a similar vein, the rural–urban fringe area currently transforms into an urban area during designated times. The years 1991–2021 are indicated by a high SUHI by the colour green to blue. Planning for smart cities is now even more important for future environmental progress. The focus of this investigation is to raise the necessary awareness among those who can lessen the challenges (Figure 14). The SUHI measurements are further significant in support of urbanization examination and estimation of the general environmental situation. Consequently, the SUHI dimension and assessment of the thermal difference over the urbanized regions were additionally vital. The global urbanization and changing climate influences of the KMC megacity, settlement, and city sites are a cumulative phenomenon that is activating the environmental variables and health problems. Those circumstances are essential for wide valuation and organization; climatic circumstances affect the general Earth’s surface and increase the risk of thermal variation. In addition, unplanned metropolises were frequently affected by the SUHI variation because numerous countries were knowledgeable about unexpected urbanization which activated the heat island influence over the sphere. The highest SUHI values observed were 3.21 (1991), 3.49 (1996), 3.66 (2001), 3.90 (2006), 4.37 (2016), and 4.56 (2021), respectively. The SUHI increased by 1.25 over 30 years, while the affected areas were Khidirpur port, Dharmotola, Kalighat, Sealdha, Sovabazar, and Ultadanga areas. Similarly, for the ecological diversity assessment, UTFVI information was applied. The values of UTFVI were 0.20 (1991), 0.21 (1996), 0.24 (2001), 0.26 (2006), 0.26 (2016), and 0.26 (2021), respectively. Most of the KMC areas were affected by heat effects and thermal variation. Therefore, that information is more helpful for decision-making and future management and adaptation strategies. With the diversity and dynamic growth of built-up morphology and urban surface cover, the traditional method of examining the temporal pattern of LST to investigate UHI has lost some of its significance. Rather, the Local Climate Zones (LCZ) system, which divides the city into areas according to building height, density, and forms of land cover that interact differently with the microclimate, emerged as a strong

substitute [57]. Meanwhile, urban surfaces act as large heat energy reservoirs due to their high thermal inertia, which could have accelerated the heat flux from the Earth. In Kolkata, the noon UHI effect is not as severe or strong because of the thermal characteristics of the urban surface, which influence the daytime UHI impacts. However, because there is no direct solar heating during the night, the situation is reversed and local-scale convection stops [58].

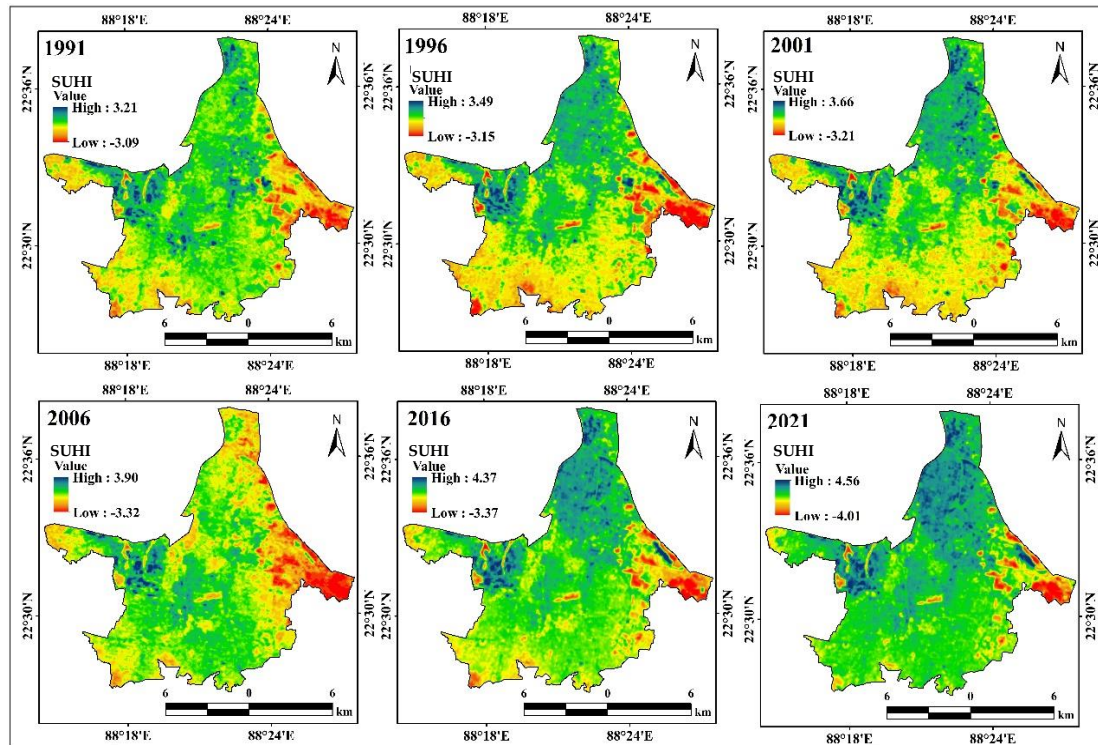


Figure 13. Maps of the SUHI in different years (1991–2021).

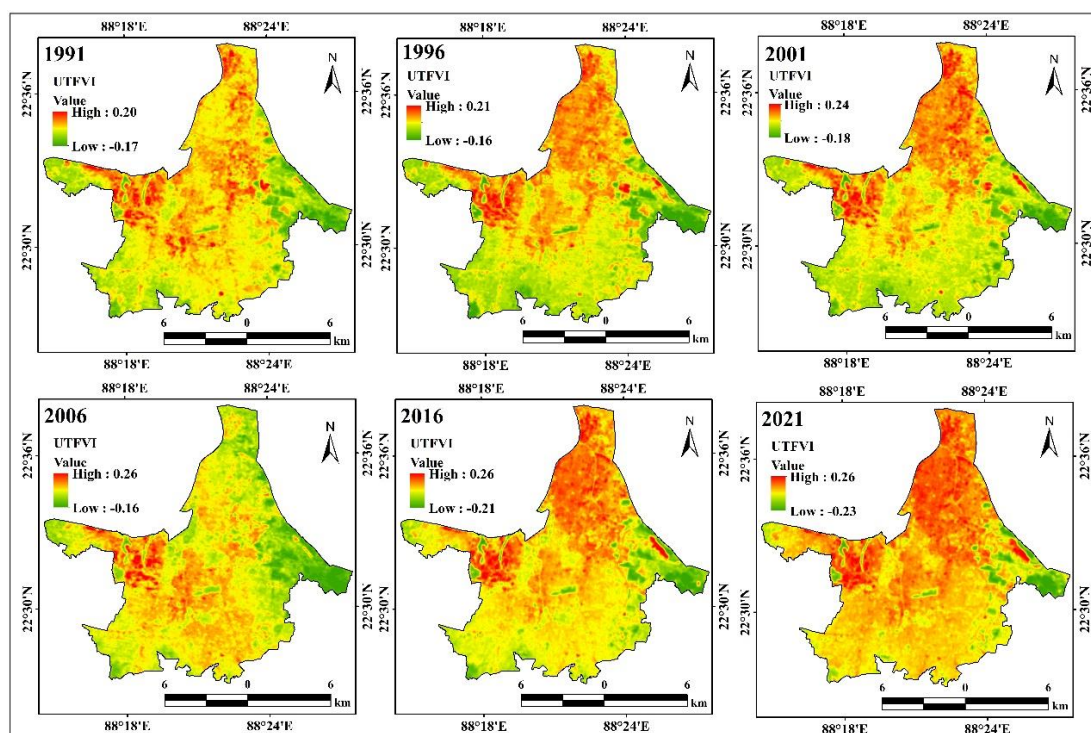


Figure 14. Maps of the UTFVI in different years (1991–2021).

3.5. Correlation Analysis

The association between the LST and LULC diagram is caused by the green space region showing a slightly lower temperature than built-up land. The thermal difference is different for diverse LULC features. The built-up area is hotter than the rest, and the water body is colder. The association is projected to apply the ArcGIS software v10.8 and calculate the situation in different years of this examining part. The built-up area is hotter than the rest of the water body, which is quite cool and the R^2 standards are 0.32, 0.36, 0.32, 0.22, 0.24, and 0.20 in the years 1991, 1996, 2001, 2006, 2016, and 2021 correspondingly. Because of the building degradation, the green space land, and the reasons for the significant temperature difference on this site, there is an additional side correlation with LST and NDVI that is negative. The relationship between LST and NDVI is 0.07, 0.13, 0.13, 0.03, 0.05, and 0.01 in the years 1991, 1996, 2001, 2006, 2016, and 2021, respectively. Because of the high frequency of deforestation and the increase in LST over the examined region, the NDMI standards demonstrated a negative connection with LST. The R^2 standards are 0.32, 0.36, 0.32, 0.22, 0.24, and 0.20 in the years 1991, 1996, 2001, 2006, 2016, and 2021, respectively (Figure 15). The correlation with LST and NDWI shows a positive relationship and the R^2 values are 0.03, 0.06, 0.07, 0.004, 0.02, and 0.002 in the years 1991, 1996, 2001, 2006, 2016, and 2021 correspondingly. Additionally, there was a positive association with LST as a result of the correlation with NDBal.

The dynamic relationship between LST and plant cover (NDVI) and built-up (NDBI) area is also investigated, demonstrating how vegetation cools the city's microclimate while the built-up area plays a heating role. A top-down method for verifying the effect of shifting land use on LST is offered: a microscale study with grids. The conversion of natural and agricultural lands into built-up areas is one of the main causes of the significant rise in urban hotspots in the city's southern and central regions in 2019 [59]. In contrast to NIR reflectance, which is only related to leaf structure and dry matter, SWIR reflectance is related to both leaf structure and water content. Therefore, differences in leaf internal structure are cancelled out by spectral indices employing the NIR and SWIR bands, which increases the accuracy of vegetation water content detection. Reduced leaf water content would limit transpiration, resulting in less water evaporating from the leaf surface, decreasing cooling and raising leaf temperature [60,61]. Due to their capacity to detect the water content of vegetation, the indices that use SWIR and LST have strong connections that could indicate drought-like situations during heatwaves. It has been observed that surfaces with sparse vegetation experience water stress during heatwaves; this could prevent or reverse the cooling effect of vegetation since there is less water available for plant transpiration and drying out [62].

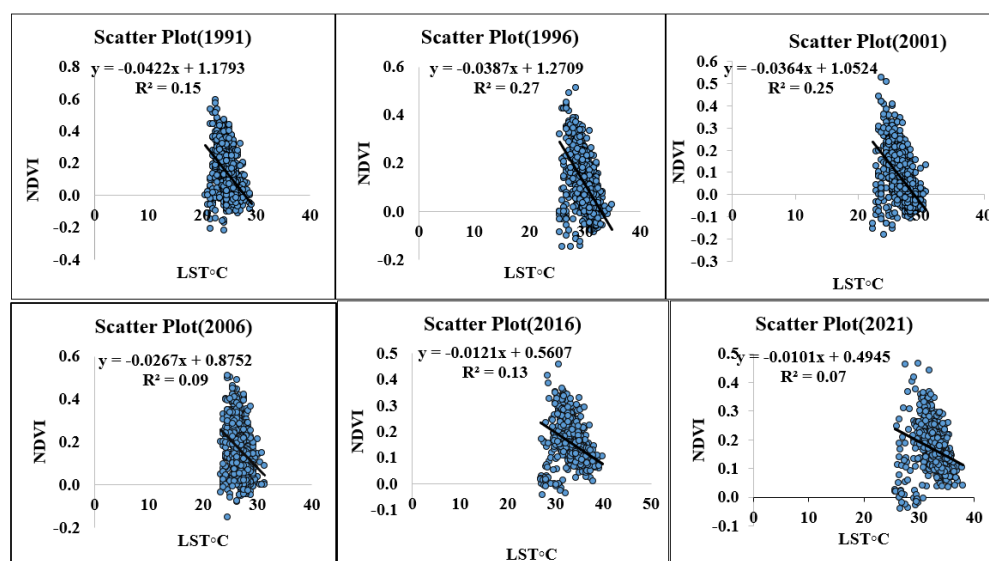


Figure 15. Cont.

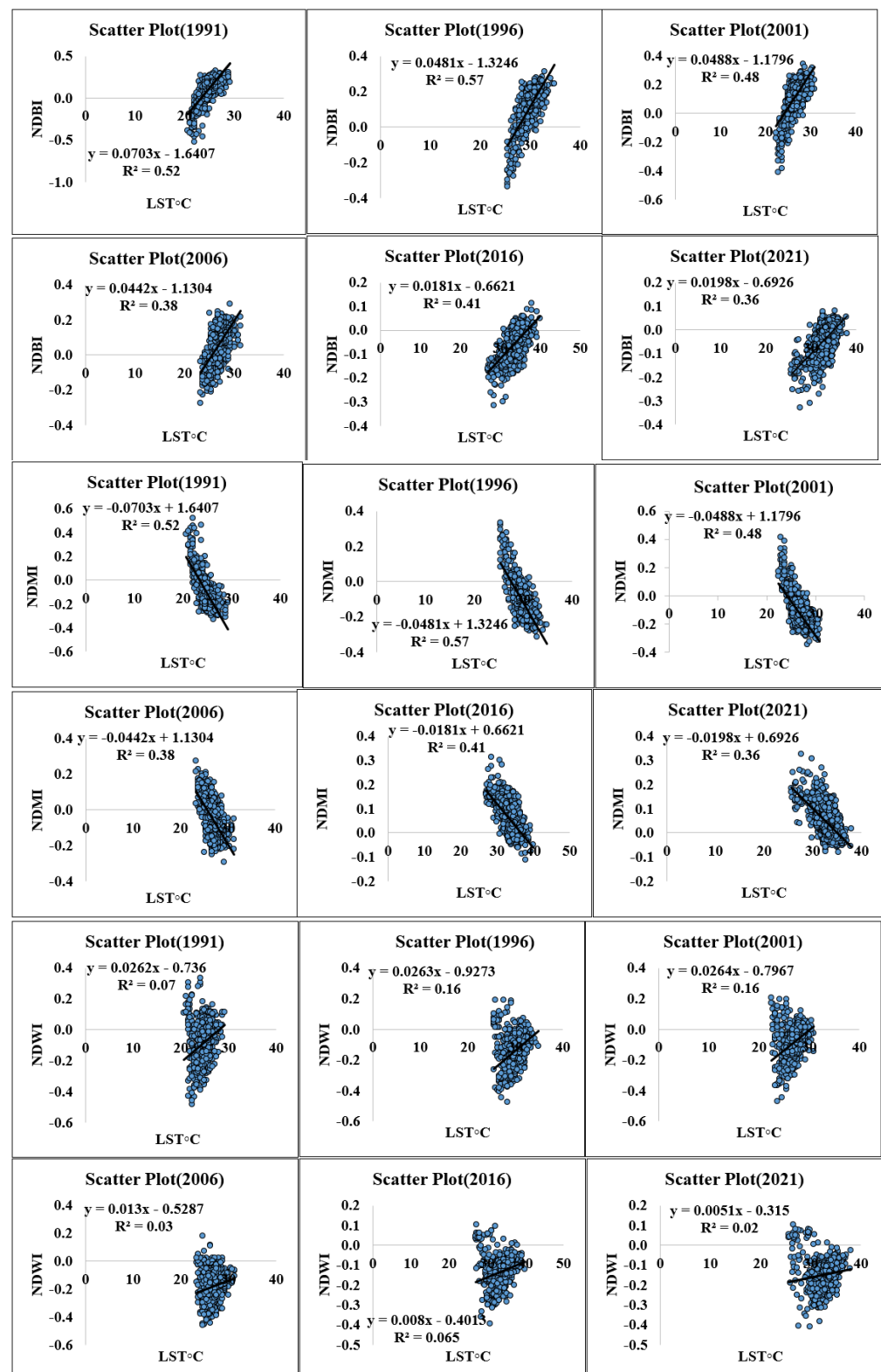


Figure 15. Cont.

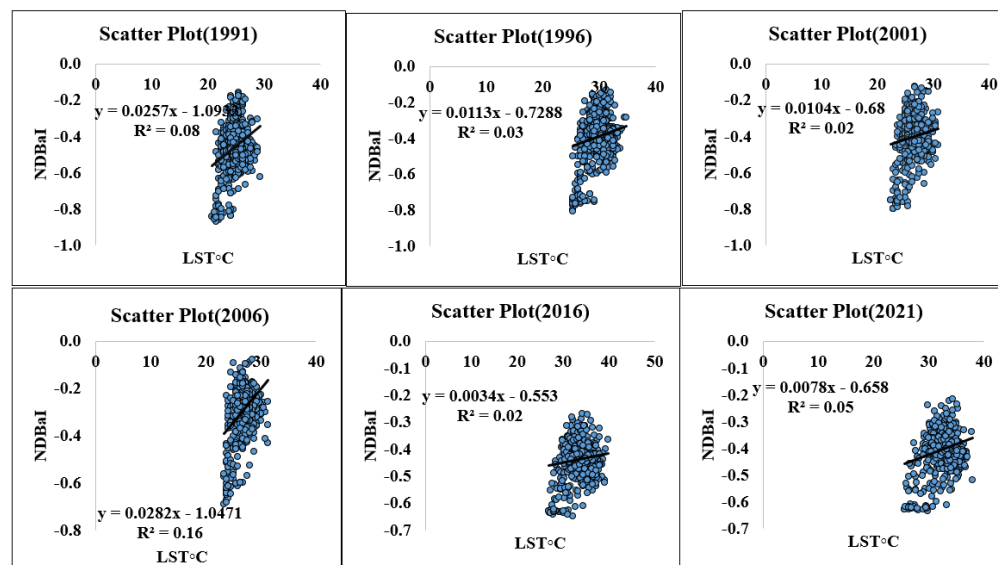


Figure 15. Correlation analysis of LST and some geo-spatial indices in different years (1991–2021).

3.6. Limitations and Recommendation

Because the satellites were capturing the images from satellite orbit, there is a distinction between surface SUHI and atmospheric SUHI. Two other factors that were crucial to examine in the upcoming research are timing and cloud cover. The massive space between the satellite location and the urban area might decrease the sensor's efficacy as there is still a substantial inconsistency between the predicted and real air temperatures [63]. It is possible that the 30 m resolution Landsat files will not be sufficient for accurately classifying the picture. The land alteration investigation's primary challenges are mixed pixels and heterogeneous values, which will make the issues in the urban expansion study worse. The upcoming research establishes the need for real surface temperatures, enhanced radiation adaption and filtering models, and Earth observation satellite systems. Aside from that, the study regions' urban green space (UGS) analysis should be conducted to advance sustainable urban design and management.

4. Conclusions

In this examination, a positive connection is found between LULC features and the LST because of the urbanization growth, industrialization, and population. An increasing LST trend is experiential from the years 1991 to 2021. The outcomes demonstrate that an increase of 4729.23 Ha in built-up areas is observed in the examining region. Temporarily, 1354.86 Ha of vegetation land, 653.31 Ha of bare land, 2286.9 Ha of grassland, and 434.16 Ha of water body region reduced from the year 1991 until 2021. Both the RS and GIS methods contribute to the main benefit of the spatio-temporal urban sprawls trend with SUHI, which, when applied as the main important impact on behalf of suitable urbanized and transportation growth, as well as ecological organization difficulties like high LST in the urbanized regions, produces SUHI; consistently, we can differentiate the UTFVI.

- The UHI and LULC results commend the significant strengthening in residential regions, similar to the temperature of the urbanized regions in the last three periods, as supplementary to added LULC features. The local thermal shape of the natural surroundings appears to have been impacted by the urbanization process, according to correlations found between LST and NDBI, NDVI, NDWI, NDMI, and NDBaI.
- The significant positive link found between LST and NDBI suggests that rapid urban growth has directly impacted the region under investigation's temperature conditions. Moreover, an inverse relationship between the decline in green space and the urban thermal field is suggested by the negative correlation between LST and NDVI.

- The primary regulating factor for SUHI and heat stress in Kolkata and the surrounding area, according to this study, is surface area. Policymakers, administrators, urban planners, and other interested parties can use this analysis for project management and planning that will reduce thermal variance and land modification over the KMC regions.

Author Contributions: Conceptualization, N.G., B.H. and J.B.; methodology, N.G., B.H., A.H.M. and T.M.T.L.; software, N.G. and B.H.; validation, B.H., J.B., M.F.A., A.H.M. and T.M.T.L.; formal analysis, N.G., B.H., J.B., M.F.A., A.H.M. and T.M.T.L.; investigation, N.G., B.H., J.B., M.F.A., A.H.M. and T.M.T.L.; resources, A.H.M. and T.M.T.L.; data curation, N.G., B.H., A.H.M. and M.F.A.; writing—original draft preparation, N.G., B.H., J.B., A.H.M., M.F.A. and T.M.T.L.; writing—review and editing, N.G., B.H., J.B., M.F.A., A.H.M. and T.M.T.L.; visualization, B.H., A.H.M. and T.M.T.L.; supervision, J.B., B.H. and T.M.T.L.; project administration, A.H.M. and T.M.T.L.; funding acquisition, A.H.M. and T.M.T.L. All authors have read and agreed to the published version of the manuscript.

Funding: This research received no external funding.

Institutional Review Board Statement: Not applicable.

Informed Consent Statement: Not applicable.

Data Availability Statement: Data will be supplied upon request from the corresponding author.

Acknowledgments: The authors are thankful to the Vidyasagar University for this research opportunity and truly thankful to the local government body for the field survey and data collection.

Conflicts of Interest: The authors declare no conflict of interest.

References

1. Ishola, K.A.; Okogbue, E.C.; Adeyeri, O.E. Dynamics of Surface Urban Biophysical Compositions and Its Impact on Land Surface Thermal Field. *Model. Earth Syst. Environ.* **2016**, *2*, 1–20. [\[CrossRef\]](#)
2. Atef, I.; Ahmed, W.; Abdel-Maguid, R.H. Modelling of Land Use Land Cover Changes Using Machine Learning and GIS Techniques: A Case Study in El-Fayoum Governorate, Egypt. *Environ. Monit. Assess.* **2023**, *195*, 637. [\[CrossRef\]](#) [\[PubMed\]](#)
3. Armanuos, A.; Ahmed, K.; Sanusi Shiru, M.; Jamei, M. Impact of Increasing Pumping Discharge on Groundwater Level in the Nile Delta Aquifer, Egypt. *Knowl.-Based Eng. Sci.* **2021**, *2*, 13–23. [\[CrossRef\]](#)
4. Zhang, S.; Omar, A.H.; Hashim, A.S.; Alam, T.; Khalifa, H.A.E.-W.; Elkotb, M.A. Enhancing Waste Management and Prediction of Water Quality in the Sustainable Urban Environment Using Optimized Algorithm of Least Square Support Vector Machine and Deep Learning Techniques. *Urban Clim.* **2023**, *49*, 101487. [\[CrossRef\]](#)
5. Voogt, J.A.; Oke, T.R. Thermal Remote Sensing of Urban Climates. *Remote Sens. Environ.* **2003**, *86*, 370–384. [\[CrossRef\]](#)
6. Lu, D.; Weng, Q. Use of Impervious Surface in Urban Land-Use Classification. *Remote Sens. Environ.* **2006**, *102*, 146–160. [\[CrossRef\]](#)
7. Sarrat, C.; Lemonsu, A.; Masson, V.; Guedalia, D. Impact of Urban Heat Island on Regional Atmospheric Pollution. *Atmos. Environ.* **2006**, *40*, 1743–1758. [\[CrossRef\]](#)
8. Abd Alraheem, E.; Jaber, N.A.; Jamei, M.; Tangang, F. Assessment of Future Meteorological Drought under Representative Concentration Pathways (RCP8. 5) Scenario: Case Study of Iraq. *Knowl.-Based Eng. Sci.* **2022**, *3*, 64–82.
9. Mundia, C.N.; James, M.M. Dynamism of Land Use Changes on Surface Temperature in Kenya: A Case Study of Nairobi City. *Int. J. Sci. Res.* **2014**, *3*, 38–41.
10. Avdan, U.; Jovanovska, G. Algorithm for Automated Mapping of Land Surface Temperature Using LANDSAT 8 Satellite Data. *J. Sens.* **2016**, *2016*, 1480307. [\[CrossRef\]](#)
11. Cheruto, M.C.; Kauti, M.K.; Kisangau, D.P.; Kariuki, P.C. Assessment of Land Use and Land Cover Change Using GIS and Remote Sensing Techniques: A Case Study of Makueni County, Kenya. *J. Remote. Sens. GIS* **2016**, *5*, 1000175. [\[CrossRef\]](#)
12. Meer, M.S.; Mishra, A.K. Land Use/Land Cover Changes over a District in Northern India Using Remote Sensing and GIS and Their Impact on Society and Environment. *J. Geol. Soc. India* **2020**, *95*, 179–182. [\[CrossRef\]](#)
13. Estoque, R.C.; Murayama, Y.; Myint, S.W. Effects of Landscape Composition and Pattern on Land Surface Temperature: An Urban Heat Island Study in the Megacities of Southeast Asia. *Sci. Total Environ.* **2017**, *577*, 349–359. [\[CrossRef\]](#) [\[PubMed\]](#)
14. Gohain, K.J.; Mohammad, P.; Goswami, A. Assessing the Impact of Land Use Land Cover Changes on Land Surface Temperature over Pune City, India. *Quat. Int.* **2021**, *575*, 259–269. [\[CrossRef\]](#)
15. Mahmoud, A.A.; Mbengue, M.T.M.; Hussain, S.; Abdullahi, M.A.; Beddal, D.; Abba, S.I. Investigation for Flood Flow Quantification of Porous Asphalt with Different Surface and Subsurface Thickness. *Knowl.-Based Eng. Sci.* **2023**, *4*, 78–89.
16. Zheng, B.; Myint, S.W.; Fan, C. Spatial Configuration of Anthropogenic Land Cover Impacts on Urban Warming. *Landsc. Urban Plan.* **2014**, *130*, 104–111. [\[CrossRef\]](#)
17. Kumar, R.; Raj Gautam, H. Climate Change and Its Impact on Agricultural Productivity in India. *J. Climatol. Weather Forecast.* **2014**, *2*, 1000109. [\[CrossRef\]](#)

18. Saleem, M.; Iqbal, J.; Shah, M.H. Non-Carcinogenic and Carcinogenic Health Risk Assessment of Selected Metals in Soil around a Natural Water Reservoir, Pakistan. *Ecotoxicol. Environ. Saf.* **2014**, *108*, 42–51. [\[CrossRef\]](#)
19. Chakraborty, T.; Hsu, A.; Many, D.; Sherif, G. A Spatially Explicit Surface Urban Heat Island Database for the United States: Characterization, Uncertainties, and Possible Applications. *ISPRS J. Photogramm. Remote Sens.* **2020**, *168*, 74–88. [\[CrossRef\]](#)
20. Shahmohamadi, P.; Che-Ani, A.I.; Etessam, I.; Maulud, K.N.A.; Tawil, N.M. Healthy Environment: The Need to Mitigate Urban Heat Island Effects on Human Health. *Procedia Eng.* **2011**, *20*, 61–70. [\[CrossRef\]](#)
21. Gupta, K.; Kumar, P.; Pathan, S.K.; Sharma, K.P. Urban Neighborhood Green Index—A Measure of Green Spaces in Urban Areas. *Landsc. Urban Plan.* **2012**, *105*, 325–335. [\[CrossRef\]](#)
22. Veettil, B.K.; Grondona, A.E.B. Vegetation Changes and Formation of Small-Scale Urban Heat Islands in Three Populated Districts of Kerala State, India. *Acta Geophys.* **2018**, *66*, 1063–1072. [\[CrossRef\]](#)
23. Hashim, B.M.; Sultan, M.A.; Attyia, M.N.; Al Maliki, A.A.; Al-Ansari, N. Change Detection and Impact of Climate Changes to Iraqi Southern Marshes Using Landsat 2 Mss, Landsat 8 Oli and Sentinel 2 Msi Data and Gis Applications. *Appl. Sci.* **2019**, *9*, 2016. [\[CrossRef\]](#)
24. Jamei, M.; Ali, M.; Jun, C.; Bateni, S.M.; Karbasi, M.; Farooque, A.A.; Yaseen, Z.M. Multi-Step Ahead Hourly Forecasting of Air Quality Indices in Australia: Application of an Optimal Time-Varying Decomposition-Based Ensemble Deep Learning Algorithm. *Atmos. Pollut. Res.* **2023**, *14*, 101752. [\[CrossRef\]](#)
25. Yu, X.; Guo, X.; Wu, Z. Land Surface Temperature Retrieval from Landsat 8 TIRS—Comparison between Radiative Transfer Equation-Based Method, Split Window Algorithm and Single Channel Method. *Remote Sens.* **2014**, *6*, 9829–9852. [\[CrossRef\]](#)
26. Ke, Y.; Im, J.; Lee, J.; Gong, H.; Ryu, Y. Characteristics of Landsat 8 OLI-Derived NDVI by Comparison with Multiple Satellite Sensors and In-Situ Observations. *Remote Sens. Environ.* **2015**, *164*, 298–313. [\[CrossRef\]](#)
27. Sekertekin, A.; Bonafoni, S. Land Surface Temperature Retrieval from Landsat 5, 7, and 8 over Rural Areas: Assessment of Different Retrieval Algorithms and Emissivity Models and Toolbox Implementation. *Remote Sens.* **2020**, *12*, 294. [\[CrossRef\]](#)
28. Carlsson, T. An Overview of the “Triangle Method” for Estimating Surface Evapotranspiration and Soil Moisture from Satellite Imagery. *Sensors* **2007**, *7*, 1612–1629. [\[CrossRef\]](#)
29. Omran, E.-S.E. Detection of Land-Use and Surface Temperature Change at Different Resolutions. *J. Geogr. Inf. Syst.* **2012**, *4*, 189–203. [\[CrossRef\]](#)
30. Orhan, O.; Ekercin, S.; Dadaser-Celik, F. Use of Landsat Land Surface Temperature and Vegetation Indices for Monitoring Drought in the Salt Lake Basin Area, Turkey. *Sci. World J.* **2014**, *2014*, 142939. [\[CrossRef\]](#)
31. Berwal, S.; Kumar, D.; Pandey, A.K.; Singh, V.P.; Kumar, R.; Kumar, K. Dynamics of Thermal Inertia over Highly Urban City: A Case Study of Delhi. In *Remote Sensing Technologies and Applications in Urban Environments*; SPIE: Bellingham, WA, USA, 2016; Volume 10008, pp. 108–114.
32. Kayet, N.; Pathak, K.; Chakrabarty, A.; Sahoo, S. Spatial Impact of Land Use/Land Cover Change on Surface Temperature Distribution in Saranda Forest, Jharkhand. *Model. Earth Syst. Environ.* **2016**, *2*, 127. [\[CrossRef\]](#)
33. Jensen Mausel, P.; Dias, N.; Gonser, R.; Yang, C.; Everitt, J.; Fletcher, R. Spectral Analysis of Coastal Vegetation and Land Cover Using AISA+ Hyperspectral Data. *Geocarto Int.* **2007**, *22*, 17–28. [\[CrossRef\]](#)
34. Cohen, J. Weighted Kappa: Nominal Scale Agreement Provision for Scaled Disagreement or Partial Credit. *Psychol. Bull.* **1968**, *70*, 213. [\[CrossRef\]](#) [\[PubMed\]](#)
35. Zoungrana, B.J.B.; Conrad, C.; Thiel, M.; Amekudzi, L.K.; Da, E.D. MODIS NDVI Trends and Fractional Land Cover Change for Improved Assessments of Vegetation Degradation in Burkina Faso, West Africa. *J. Arid Environ.* **2018**, *153*, 66–75. [\[CrossRef\]](#)
36. Li, Q.; Zhang, T.; Yu, Y. Using Cloud Computing to Process Intensive Floating Car Data for Urban Traffic Surveillance. *Int. J. Geogr. Inf. Sci.* **2011**, *25*, 1303–1322. [\[CrossRef\]](#)
37. Jin, Z.; Zhang, L.; Lv, J.; Sun, X. The Application of Geostatistical Analysis and Receptor Model for the Spatial Distribution and Sources of Potentially Toxic Elements in Soils. *Environ. Geochem. Health* **2021**, *43*, 407–421. [\[CrossRef\]](#) [\[PubMed\]](#)
38. Sobrino, J.A.; Raissouni, N.; Li, Z.-L. A Comparative Study of Land Surface Emissivity Retrieval from NOAA Data. *Remote Sens. Environ.* **2001**, *75*, 256–266. [\[CrossRef\]](#)
39. Guha, S.; Govil, H.; Dey, A.; Gill, N. Analytical Study of Land Surface Temperature with NDVI and NDBI Using Landsat 8 OLI and TIRS Data in Florence and Naples City, Italy. *Eur. J. Remote Sens.* **2018**, *51*, 667–678. [\[CrossRef\]](#)
40. Singh, P.; Kikon, N.; Verma, P. Impact of Land Use Change and Urbanization on Urban Heat Island in Lucknow City, Central India. A Remote Sensing Based Estimate. *Sustain. Cities Soc.* **2017**, *32*, 100–114. [\[CrossRef\]](#)
41. Kedia, S.; Bhakare, S.P.; Dwivedi, A.K.; Islam, S.; Kaginalkar, A. Estimates of Change in Surface Meteorology and Urban Heat Island over Northwest India: Impact of Urbanization. *Urban Clim.* **2021**, *36*, 100782. [\[CrossRef\]](#)
42. Chandler, T.J. Urban Climatology and Urban Planning. *Geogr. J.* **1976**, *142*, 57. [\[CrossRef\]](#)
43. Estoque, R.C.; Murayama, Y. Monitoring Surface Urban Heat Island Formation in a Tropical Mountain City Using Landsat Data (1987–2015). *ISPRS J. Photogramm. Remote Sens.* **2017**, *133*, 18–29. [\[CrossRef\]](#)
44. Zhao, H.; Chen, X. Use of Normalized Difference Bareness Index in Quickly Mapping Bare Areas from TM/ETM+. In Proceedings of the International Geoscience and Remote Sensing Symposium, Seoul, Republic of Korea, 29 July 2005; Volume 3, p. 1666.
45. Guha, S.; Govil, H.; Besoya, M. An Investigation on Seasonal Variability between LST and NDWI in an Urban Environment Using Landsat Satellite Data. *Geomat. Nat. Hazards Risk* **2020**, *11*, 1319–1345. [\[CrossRef\]](#)

46. Sobrino, J.A.; Jiménez-Muñoz, J.C.; Paolini, L. Land Surface Temperature Retrieval from LANDSAT TM 5. *Remote Sens. Environ.* **2004**, *90*, 434–440. [\[CrossRef\]](#)
47. Scarano, M.; Sobrino, J.A. On the Relationship between the Sky View Factor and the Land Surface Temperature Derived by Landsat-8 Images in Bari, Italy. *Int. J. Remote Sens.* **2015**, *36*, 4820–4835. [\[CrossRef\]](#)
48. Mirzaei, P.A.; Haghighat, F. Approaches to Study Urban Heat Island—Abilities and Limitations. *Build. Environ.* **2010**, *45*, 2192–2201. [\[CrossRef\]](#)
49. Abir, F.A.; Ahmmed, S.; Sarker, S.H.; Fahim, A.U. Thermal and Ecological Assessment Based on Land Surface Temperature and Quantifying Multivariate Controlling Factors in Bogura, Bangladesh. *Heliyon* **2021**, *7*, e08012. [\[CrossRef\]](#) [\[PubMed\]](#)
50. Ray, R.; Das, A.; Hasan, M.S.U.; Aldrees, A.; Islam, S.; Khan, M.A.; Lama, G.F.C. Quantitative Analysis of Land Use and Land Cover Dynamics Using Geoinformatics Techniques: A Case Study on Kolkata Metropolitan Development Authority (KMDA) in West Bengal, India. *Remote Sens.* **2023**, *15*, 959. [\[CrossRef\]](#)
51. Sharma, R.; Chakraborty, A.; Joshi, P.K. Geospatial Quantification and Analysis of Environmental Changes in Urbanizing City of Kolkata (India). *Environ. Monit. Assess.* **2015**, *187*, 4206. [\[CrossRef\]](#)
52. Hasnine, M.; Rukhsana. Spatial and Temporal Analysis of Land Use and Land Cover Change in and around Kolkata City, India, Using Geospatial Techniques. *J. Indian Soc. Remote Sens.* **2023**, *51*, 1037–1056. [\[CrossRef\]](#)
53. Das, P.; Vamsi, K.S.; Zhenke, Z. Decadal Variation of the Land Surface Temperatures (LST) and Urban Heat Island (UHI) over Kolkata City Projected Using MODIS and ERA-Interim DataSets. *Aerosol Sci. Eng.* **2020**, *4*, 200–209. [\[CrossRef\]](#)
54. Biswas, S.; Ghosh, S. Estimation of Land Surface Temperature in Response to Land Use/Land Cover Transformation in Kolkata City and Its Suburban Area, India. *Int. J. Urban Sci.* **2022**, *26*, 604–631. [\[CrossRef\]](#)
55. Ali, M.B.; Jamal, S.; Ahmad, M.; Saqib, M. Unriddle the Complex Associations among Urban Green Cover, Built-up Index, and Surface Temperature Using Geospatial Approach: A Micro-Level Study of Kolkata Municipal Corporation for Sustainable City. *Theor. Appl. Climatol.* **2024**, 1–22. [\[CrossRef\]](#)
56. Lu, L.; Fu, P.; Dewan, A.; Li, Q. Contrasting Determinants of Land Surface Temperature in Three Megacities: Implications to Cool Tropical Metropolitan Regions. *Sustain. Cities Soc.* **2023**, *92*, 104505. [\[CrossRef\]](#)
57. Bhowmick, D.; Mukherjee, K.; Dash, P.; Mondal, R. Use of “Local Climate Zones” for Detecting Urban Heat Island: A Case Study of Kolkata Metropolitan Area, India. In *IOP Conference Series: Earth and Environmental Science, Proceedings of the International Conference on Geospatial Science for Digital Earth Observation (GSDEO-2021), Online, 26–27 March 2021*; IOP Publishing: Bristol, UK, 2023; Volume 1164, p. 12007.
58. Khorat, S.; Das, D.; Khatun, R.; Aziz, S.M.; Anand, P.; Khan, A.; Santamouris, M.; Niyogi, D. Cool Roof Strategies for Urban Thermal Resilience to Extreme Heatwaves in Tropical Cities. *Energy Build.* **2024**, *302*, 113751. [\[CrossRef\]](#)
59. Sharma, R.; Pradhan, L.; Kumari, M.; Bhattacharya, P. Assessing Urban Heat Islands and Thermal Comfort in Noida City Using Geospatial Technology. *Urban Clim.* **2021**, *35*, 100751. [\[CrossRef\]](#)
60. Ceccato, P.; Flasse, S.; Tarantola, S.; Jacquemoud, S.; Grégoire, J.-M. Detecting Vegetation Leaf Water Content Using Reflectance in the Optical Domain. *Remote Sens. Environ.* **2001**, *77*, 22–33. [\[CrossRef\]](#)
61. Yao, X.; Yu, K.; Zeng, X.; Lin, Y.; Ye, B.; Shen, X.; Liu, J. How Can Urban Parks Be Planned to Mitigate Urban Heat Island Effect in “Furnace Cities”? An Accumulation Perspective. *J. Clean. Prod.* **2022**, *330*, 129852. [\[CrossRef\]](#)
62. Alexander, C. Normalised Difference Spectral Indices and Urban Land Cover as Indicators of Land Surface Temperature (LST). *Int. J. Appl. Earth Obs. Geoinf.* **2020**, *86*, 102013. [\[CrossRef\]](#)
63. Mohamed, A.H.; Adwan, I.A.I.; Ahmeda, A.G.F.; Hrtemih, H.; Al-MSari, H. Identification of Affecting Factors on the Travel Time Reliability for Bus Transportation. *Knowl.-Based Eng. Sci.* **2021**, *2*, 19–30. [\[CrossRef\]](#)

Disclaimer/Publisher’s Note: The statements, opinions and data contained in all publications are solely those of the individual author(s) and contributor(s) and not of MDPI and/or the editor(s). MDPI and/or the editor(s) disclaim responsibility for any injury to people or property resulting from any ideas, methods, instructions or products referred to in the content.